Lithos 220–223 (2015) 133–146

Contents lists available at ScienceDirect

Lithos

journal homepage: www.elsevier.com/locate/lithos

A Neoarchean subduction polarity reversal event in the North China Craton

Junpeng Wang [a,b,c], Timothy Kusky [a,c,d,*], Lu Wang [a,c], Ali Polat [a,c,e], Hao Deng [a,c]

[a] State Key Laboratory of Geological Processes and Mineral Resources, China University of Geosciences, Wuhan 430074, China
[b] Department of Earth, Planetary, and Space Sciences, University of California, Los Angeles, CA 90095, USA
[c] Center for Global Tectonics, China University of Geosciences, Wuhan 430074, China
[d] Three Gorges Research Center for Geo-hazards, Ministry of Education, China University of Geosciences, Wuhan 430074, China
[e] Department of Earth and Environmental Sciences, University of Windsor, Windsor, ON N9B 3P4, Canada

ARTICLE INFO

Article history:
Received 23 October 2014
Accepted 22 January 2015
Available online 14 February 2015

Keywords:
Neoarchean
Subduction polarity reversal
Arc–continent collision
Zanhuang tectonic mélange
Central Orogenic Belt
North China Craton

ABSTRACT

Subduction polarity reversal events following arc–continent, arc–arc or continent–continent collisions have been well-documented from Cenozoic, Mesozoic, and Paleozoic orogens, but not from the Archean. We here document a Neoarchean subduction reversal event after an arc–continent collision between the Eastern Block of the North China Craton (NCC) and the Fuping arc using field, geochemical and geochronological data. We focus our work on the Wangjiazhuang granite in the Zanhuang massif located along the eastern margin of the Central Orogenic Belt (COB) of the NCC, and a regional tectonic comparison with other granitic rocks with similar ages, geochemical and petrogenetic characteristics. The ca. 2.5 Ga A-type Wangjiazhuang granite intrudes the Neoarchean Zanhuang mélange belt and contains mafic and felsic inclusions. It has positive $\varepsilon_{Nd}(t)$ values (+0.12 to +1.13) and T_{DM2} ages between 2784 Ma and 2869 Ma. This work shows clearly, from field structural relationships, geochemistry and geochronology, that the Wangjiazhuang granite formed after an arc–continent collision between the Eastern Block which is defined as a continental block and the Fuping arc, after a subduction polarity reversal event placed a new slab beneath the collisionally modified margin of the Eastern Block and converted it to an Andean-type margin. The subduction polarity reversal event at ca. 2.5 Ga resulted in melting of the enriched mantle. Meanwhile, the rising magma induced partial melting of the old and thickened TTG crust leading to the intrusion of ca. 2.5 Ga Wangjiazhuang granite into the Neoarchean Zanhuang mélange. There are other granitic rocks with similar ages and geochemical and petrogenetic features in the Central Orogenic Belt and Eastern Block of the North China Craton, suggesting that they formed in a similar tectonic setting as the circa 2.5 Ga granites across the Eastern Block. The Neoarchean subduction polarity reversal event and prior arc–continent collision provide strong evidence that plate tectonics was operating by the end of the Neoarchean.

1. Introduction

Subduction polarity reversal events after arc–contintent, arc–arc or continent–continent collisions have been documented in Cenozoic and Mesozoic orogens in several places in the world, such as the Ligurian Alps, Italy (Vignaroli et al., 2008), Kamchatka (NE Russia) in the northwest Pacific (Konstantinovskaia, 2001), Taiwan-Luzon (Chemenda et al., 1997; Clift et al., 2003; Teng et al., 2000; Ustaszewski et al., 2012), Cretaceous Caribbean island arc (Draper et al., 1996; Lebron and Perfit, 1993), Solomon island arc (Copper and Taylor, 1985), Philippines (Pubellier et al., 1999), and northern New Guinea (Copper and Taylor, 1987; Dewey and Bird, 1970). However, subduction polarity reversal events have not been clearly documented from the Archean rock record. In this paper, based on the field structural, geochemical and geochronological studies on the Wangjiazhuang granite and a regional tectonic synthesis of geochemical and petrogenetic data from similar-aged plutons in the NCC, we propose a Neoarchean subduction polarity reversal event following an arc–continent collision between Eastern Block and the Fuping arc in the NCC.

In the past several decades, most workers have generally divided the NCC into the Eastern Block (EB) and Western Block (WB), separated by the intervening Central Orogenic Belt (Fig. 1; Kusky and Li, 2003; Zhao et al., 2001), or several smaller microblocks (Zhai and Santosh, 2011). Currently, the amalgamation mechanism of the Precambrian basement and formation age of the NCC are a hot topic (Deng et al., 2013, 2014; Kusky et al., 2014; Lu et al., 2014; Wang et al., 2013a, 2014a,b,c,d; Xiao et al., 2014; Yin et al., 2014; Zhang et al., 2007c, 2009, 2012; Zhao et al., 2012). Circa 2.5 Ga magmatic events within the North China Craton are strongly developed with the prominent characteristics of emplacement of the granitic rocks in the late stage of the Neoarchean

* Corresponding author at: State Key Laboratory of Geological Processes and Mineral Resources, China University of Geosciences, Wuhan 430074, China.
E-mail address: tkusky@gmail.com (T. Kusky).

http://dx.doi.org/10.1016/j.lithos.2015.01.029
0024-4937/

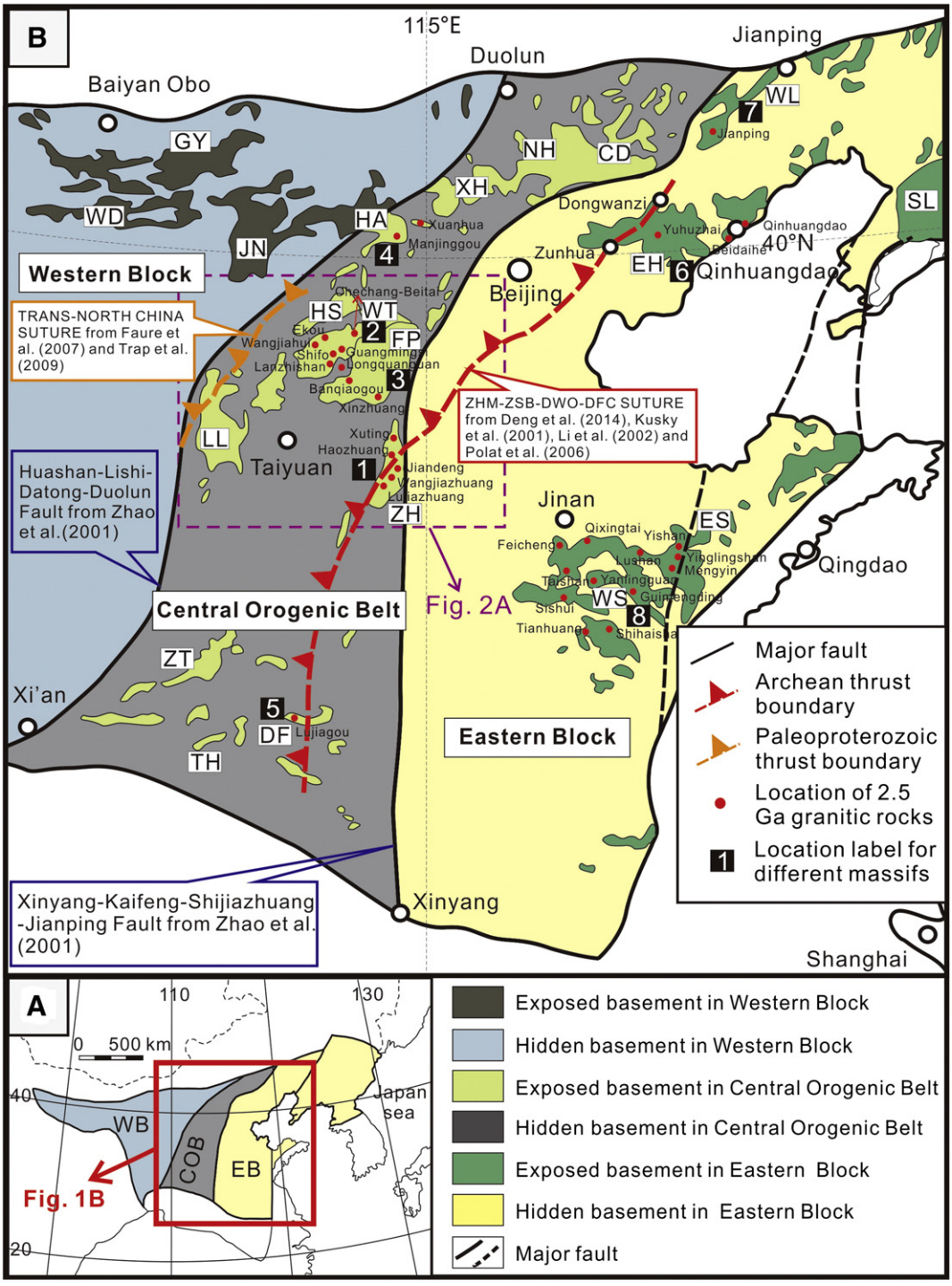

Fig. 1. A: Tectonic subdivision of the North China Craton (NCC) including Western Block (WB), Eastern Block (EB) and Central Orogenic Belt (COB). B: The distribution of the exposed basement of the central part of North China Craton with locations of Huashan–Lishi–Datong–Duolun and Xinyang–Kaifeng–Shijiazhuang–Jianping Faults from Zhao et al. (2001), Trans-North China suture from Faure et al. (2007) and Trap et al. (2009), and Zanhuang Melange (ZHM)–Zunhua Structural Belt (ZSB)–Dongwanzi Ophiolite (DWO)–Dengfeng Complex (DFC) suture from Deng et al. (2014), Kusky et al. (2001), Li et al. (2002) and Polat et al. (2006). Abbreviations of metamorphic complexes without exposure of 2.5 Ga granitic rocks: CD: Chengde; ES: Eastern Shandong Province; GY: Guyang; HS: Hengshan Complex; JN: Jining; LL: Lüliang; NH: Northern Hebei Province; SL: Southern Liaoning Province; TH: Taihua; WD: Wulashan–Daqingshan; XH: Xuanhua; and ZT: Zhongtiao Complex. Abbreviations of metamorphic complexes with exposure of 2.5 Ga granitic rocks: ZH (labeled as 1): Zanhuang Massif; WT (labeled as 2): Wutai Complex; FP (labeled as 3): Fuping Complex; HA (labeled as 4): Huai'an Complex; DF (labeled as 5): Dengfeng Complex; EH (labeled as 6): Eastern Hebei Province; WL (labeled as 7): Western Liaoning Province; and WS (labeled as 8): Western Shandong Province. Map modified from Zhao et al. (2005) and Kusky and Li (2003).

tectonic activity (Geng et al., 2010; Han et al., 2014; Ma et al., 2013; Nutman et al., 2011; Wilde et al., 2005; Zhang et al., 2013). However, the petrogenetic origin and geodynamic triggering mechanism for the 2.5 Ga magmatic event are poorly understood and controversial, with one group of thought arguing that they were related to the underplating by a mantle plume (Geng et al., 2012; Wu et al., 2014; Zhao, 2009; Zhao and Zhai, 2013; Zhao et al., 1999), whereas others favor magmatic arc models (Nutman et al., 2011; Peng et al., 2013; Wang et al., 2013b). Therefore, the study of 2.5 Ga magmatic activity in the NCC is very important and will undoubtedly provide key constraints on the early Precambrian tectonic evolution of the basement of the NCC. We previously reported that the ca. 2.5 Ga Wangjiazhuang granitic pluton intrudes the

Neoarchean Zanhuang tectonic mélange belt (see Deng et al., 2013; Wang et al., 2013a). In this paper, we present new petrographic, geochemical, LA–ICP–MS zircon U–Pb dating and Sm–Nd isotopic data from the circa 2.5 Ga Wangjiazhuang granite to constrain the formation age, magmatic source, petrogenesis, and geodynamic setting. Combined with the previous studies on the Neoarchean tectonic mélange focusing on the structures and the comparison with other ca. 2.5 Ga granitic plutons in the NCC, we aim to provide more reliable constraints on the early Precambrian tectonic evolution of the NCC.

2. Geological background

The North China Craton consisting of the Western Block, Eastern Block and Central Orogenic Belt is one of the oldest cratons worldwide (Fig. 1; Kusky and Li, 2003; Kusky et al., 2001, 2004, 2007a,b, 2014; Liu et al., 2006; Polat et al., 2005, 2006; Santosh, 2010; Wang et al., 2013a). The Central Orogenic Belt is also known as Central Belt or Trans North-China Orogen (Zhao, 2001; Zhao et al., 1999, 2001, 2002, 2005). The poorly exposed Western Block is a typical stable Archean platform with the characteristics of thick mantle root, low heat flow and few earthquakes, which is very different from the Eastern Block with high heat flow and more earthquakes resulting from the root loss of the lithosphere in the Mesozoic beneath the Eastern Block of the North China Craton (Gao et al., 2004; Griffin et al., 1998). The Central Orogenic Belt is delineated by Archean structural boundaries (Kusky, 2011b; Kusky and Li, 2003; Kusky et al., 2007a), and is generally considered to record the amalgamation of the Western Block and the Eastern Block and is crucial to understand the tectonic evolution of the whole North China Craton. TTG gneisses, circa 2.5 Ga and 2.1 Ga granites, greenschist to granulite facies supracrustal sequences, passive margin to foreland basin sedimentary rocks, 2.5–2.4 Ga and 1.9–1.7 Ga mafic dike swarms are well exposed and mainly crop out in Hengshan Massif (HS), Wutaishan Massif (WT), Fuping Massif (FP), Lüliangshan Massif (LL) and Zanghuang Massif (ZH) (Figs. 1A and 2A; Deng et al., 2013, 2014; Kröner et al., 2006; Kusky, 2011b; Kusky and Li, 2003; Kusky et al., 2007b; Peng et al., 2007; Wang et al., 2013a; Xiao and Wang, 2011).

The Zanhuang massif located on the eastern margin of the central and southern sections of the Central Orogenic Belt is one of the most important areas to study the collisional orogenesis between the Eastern Block and the Western Block of the NCC and any intervening arc terranes (Fig. 2A). Many Precambrian rocks are exposed in the Zanhuang massif, among which the Archean rocks are the most abundant. Lithologically, TTG (tonalite–trondhjemite–granodiorite) gneiss, felsic gneiss, garnet–kyanite-bearing plagioclase gneiss, garnet-bearing plagioclase amphibolite, ultramafic rocks, amphibole-plagioclase gneiss, magnetite quartzite, marble and metasandstone comprise the main rock types. Trap et al., (2009) divided the Zanhuang massif into the Western Zanhuang Domain (WZD), Eastern Zanhuang Domain (EZD) and Central Zanhuang Domain (CZD) (Fig. 2B), with a suture zone on the western margin of the Central Zanhuang Domain. They speculated that the formation of the Zanhuang massif is the result of the collision along the Taihang suture zone between the Eastern Block and Fuping arc at ca. 2150 Ma (Trap et al., 2012). We have documented a Neoarchean mélange in the Zanhuang massif of the NCC (Figs. 2B and 3A; Deng et al., 2013; Wang et al., 2013a). The Zanhuang mélange separates a passive margin to foreland basin sequence composed of a marble-siliciclastic unit developed on the western edge of the Eastern Block of the NCC from an arc terrane consisting of TTG gneisses in the Western Zanhuang Domain of Central Orogenic Belt of the NCC (Figs. 2B and 3A). The mélange contains a structurally complex tectonic mixture of metapelites, metapsammites, marbles and quartzites mixed with exotic tectonic blocks of ultramafic and metagabbroic rocks, metabasalts that locally include relict pillow structures, and TTG gneisses (Fig. 3A; Wang et al., 2013a). All units in the mélange have been intruded by mafic dikes that were subsequently deformed, and are now preserved as garnet-amphibolite boudins. These late mafic dikes are contemporaneous with the Wangjiazhuang granite that intrudes the Neoarchean Zanhuang tectonic mélange (Figs. 2B and 3; Deng et al., 2014; Wang et al., 2013a). For a detailed description of the litho-tectonic units of the mélange see Wang et al. (2013a). The formation age of rocks and tectonic structures in the mélange are constrained to be circa 2.5 Ga, and the whole mélange is cut by the 2.5 Ga granite and related pegmatites, indicating that this suture was not formed in Paleoproterozoic, but must be older than the intrusion of the cross-cutting circa 2.5 Ga granites (Deng et al., 2013; Wang et al., 2013a).

3. Field and petrographic characteristics of the Wangjiazhuang granite

The Wangjiazhuang granite has an exposed area of about 12 km^2 (Fig. 3A). It intrudes the Neoarchean Zanhuang tectonic mélange belt (Wang et al., 2013a), and has a structural contact with the Paleoproterozoic quartzite of the Guandu Group along the northern margin of the pluton. The Wangjiazhuang granite cuts the fabrics in the mélange belt, indicating that the late Archean mélange formed earlier than the Wangjiazhuang granite (Wang et al., 2013a). In addition, most of the foliation is rotated into near-parallelism with the margins of the Wangjiazhuang granite. However, the Wangjiazhuang granite truncates the earlier foliation of the mélange in the NE and SW margins of the pluton (Wang et al., 2013a). The foliation of the quartzite is parallel to the foliation of the northern edge of the granite (Fig. 4A). A small number of fine-grained mafic inclusions (Fig. 4B) and coarse-grained felsic inclusions (Fig. 4C) are present in the Wangjiazhuang granite. The edge of the granite is foliated (Fig. 4D) whereas the central part is more texturally homogeneous. Lineations defined by the orientation of elongated biotites (Fig. 4E) are well developed at the margin of the granite, whereas the quartz grains are not plastically deformed. Hence, we interpret this as a magmatic fabric (e.g., Tobisch and Patterson, 1990). The Wangjiazhuang granite truncates the early foliation in the Neoarchean Zanhuang mélange in some locations (Wang et al., 2013a). The main minerals include feldspar (55–60%), quartz (25–30%), biotite (5–10%), muscovite (<5%) and minor magnetite, apatite and zircon (Fig. 4F). Feldspar grains are mostly microcline and are variably sericitized.

4. Sampling

Seven samples of the Wangjiazhuang granite pluton were collected for major and trace element analyses from different positions within the pluton (Fig. 3A), including two samples from the northern margin the granite. From these, three samples were chosen for geochronological and isotopic analyses. All the samples are taken from the least weathered and altered outcrops in the Wangjiazhuang granite pluton.

5. Analytical methods and results

The methods of whole-rock major and trace element, zircon U–Pb dating and Sm–Nd isotopic analyses are described in the appendix (Supplementary analytical methods). The results are shown in detail below.

5.1. Zircon U–Pb geochronology and trace elements

The zircons for U–Pb dating are taken from samples 13XT17-1, 13XT19-1 and 13XT22-1 (see sample locations in Fig. 3A). The zircons from the three samples are mostly clear and euhedral grains that show internal oscillatory zoning structures in cathodoluminescence (CL) images (Supplementary Fig. 1) and no inherited cores were observed, indicating that these zircons have a magmatic origin. These characteristics above are typical for magmatic zircons in A-type granites (Wong et al., 2011; Wu and Zheng, 2004; Zhang et al., 2007a,b).

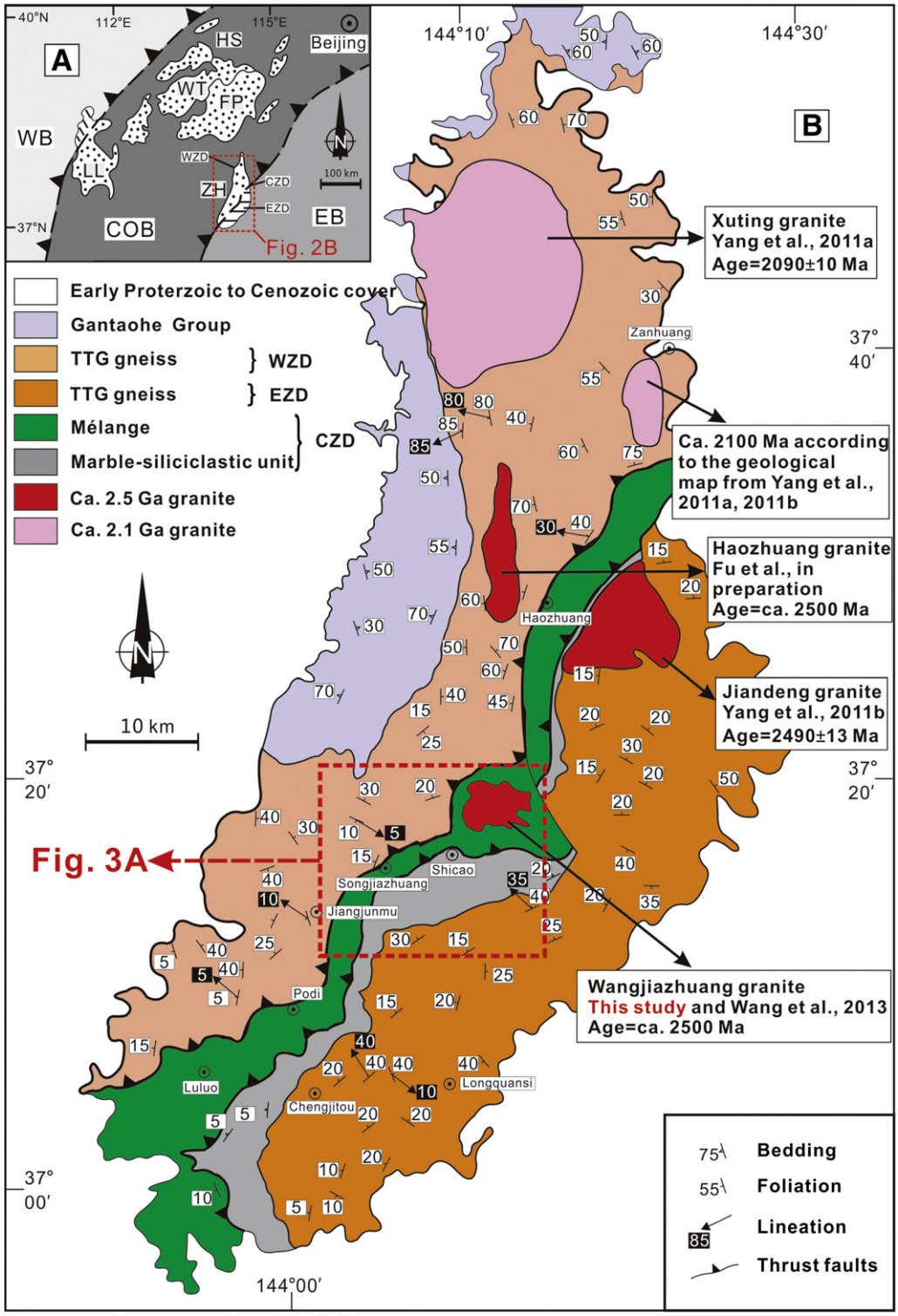

Fig. 2. A: A simple geological map of the central part of the North China Craton (NCC), showing Western Block (WB), Eastern Block (EB) and Central Orogenic Belt (COB), different massifs (Hengshan Massif = HS; Wutaishan Massif = WT; Fuping Massif = FP; Lüliangshan Massif = LL; Zanhuang Massif = ZH) within COB, and Western Zanhuang Domain (WZD), Central Zanhuang Domain (CZD), and Eastern Zanhuang Domain (EZD) of Zanhuang Massif. Map modified after Trap et al. (2009). The thrusts dipping to the northwest are interpreted as two suture zones by Faure et al. (2007), Kusky (2011a, 2011b) and Trap et al. (2009). B: Proposed geological map of the Zanhuang Massif, including the Western Zanhuang Domain consisting of TTG gneisses, Central Zanhuang Domain composed of Zanhuang mélange and marble-siliciclastic unit and Eastern Zanhuang Domain consisting of TTG gneisses. Summary of granites with different ages described in different literatures are shown in this figure. Map modified after Trap et al. (2009) and Yang et al. (2011a, 2011b).

Twenty one, 20 and 25 spots were analyzed for samples 13XT17-1, 13XT19-1 and 13XT22-1, respectively. The detailed zircon U–Pb dating results are given in Supplementary Table 1. All the U–Pb dating results of the three samples are located on or near the concordia line and within analyses errors (Fig. 5; Supplementary Table 1). The weighted mean $^{207}Pb/^{206}Pb$ age for the 21 measuring points of sample 13XT17-1 yields a relatively older age of 2517 ± 20 Ma (Fig. 5A). Twenty and 25 measuring points yield good discordant lines with weighted mean ages of 2506 ± 10 Ma (Fig. 5B; MSWD = 0.56) and 2513 ± 13 Ma (Fig. 5C; MSWD = 1.9), respectively. Twenty one, 20 and 25 rare earth element

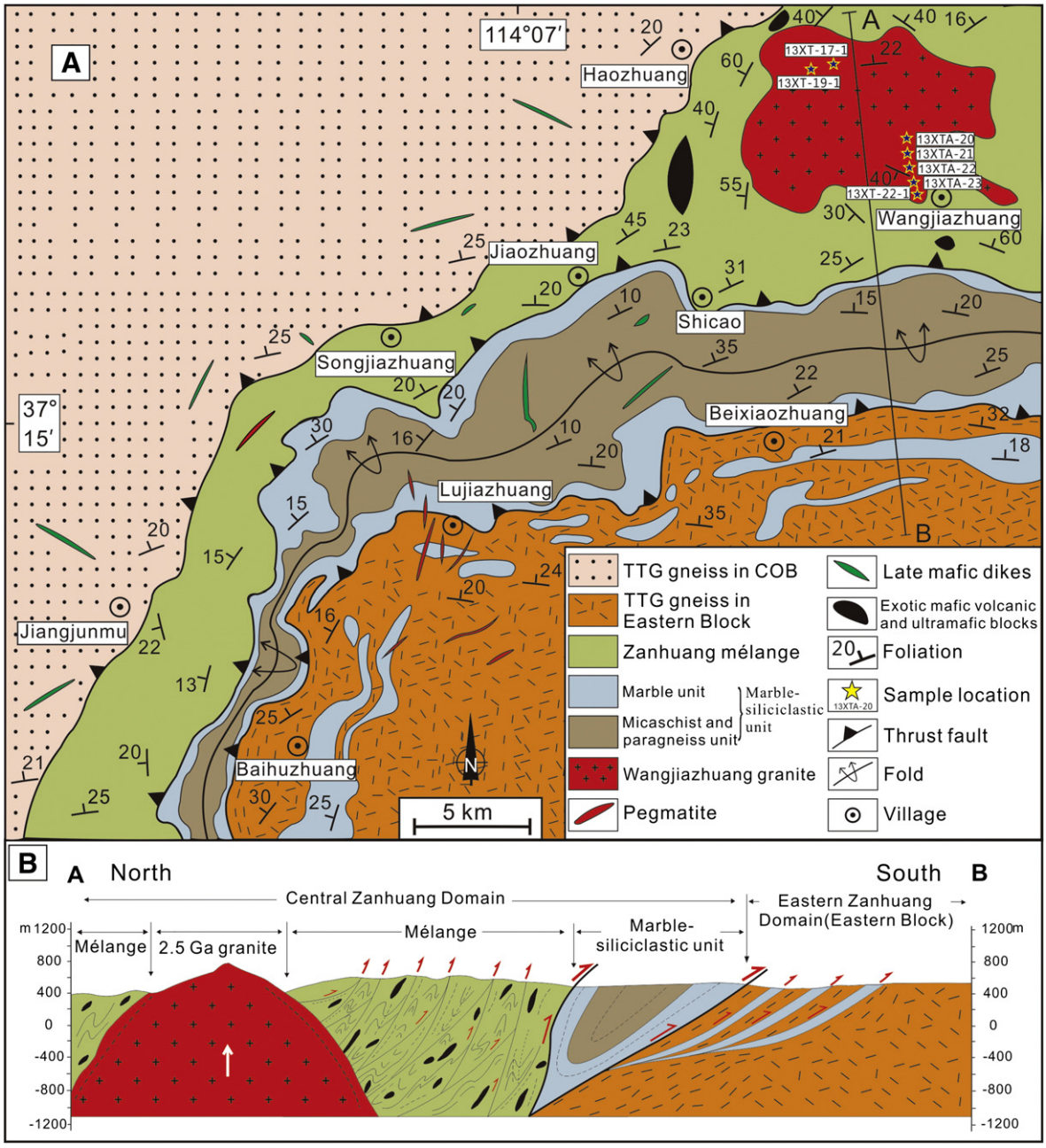

Fig. 3. A: Geological map of the study area, showing different units of the study area, including the TTG gneisses of the Western Zanhuang Domain and Eastern Block, the Neoarchean mélange belt, marble unit and mica schist and paragneiss unit of the marble-siliciclastic unit; the mélange is intruded by the Wangjiazhuang granitic pluton with surrounding schist, marble, quartzite and volcanic rocks and cross-cut by undeformed pegmatites. The mélange belt corresponds to the southeastern (Taihang) suture in panel Fig. 2A. Map modified after Wang et al. (2013a). B: Interpretive cross-section A–B through Central Zanhuang Domain to Eastern Zanhuang Domain. Note that the Central Zanhuang Domain including the mélange unit and the marble-siliciclastic unit was thrust to the southeast upon the Eastern Zanhuang Domain. The ca. 2.5 Ga granitic pluton and pegmatite intrude the Zanhuang mélange and late mafic dikes cross-cutting all units of the study area. Profile location shown in Fig. 3A, maps modified after Wang et al. (2013a).

contents were simultaneously obtained for zircons from samples 13XT17-1, 13XT19-1 and 13XT22-1 during zircon U–Pb dating (Supplementary Table 2). Chondrite-normalized REE and trace element patterns of all the zircons from the three samples show HREE enrichment, positive Ce anomalies and moderate negative Eu anomalies (Supplementary Fig. 2).

5.2. Whole-rock major and trace elements

A total of 7 samples from the Wangjiazhuang granite have been analyzed for major and trace element analyses. The major oxides described below are recalculated to 100% on a volatile-free basis. The results and related parameters are shown in Supplementary Table 3. The sample locations are shown in Fig. 3A and GPS locations are shown in Supplementary Table 3.

The Wangjiazhuang granite has a relatively narrow range of geochemical compositions, with high SiO_2 between 72.6 wt.% and 74.6 wt.%, high Al_2O_3 between 13.2 wt.% and 13.6 wt.%, MgO between 0.30 wt.% and 0.50 wt.%, $Fe_2O_3^T$ between 1.84 wt.% and 2.60 wt.%, and CaO between 0.53 wt.% and 1.16 wt.%. As shown in Supplementary Table 3, these rocks are relatively rich in alkalis with K_2O of 5.3–6.0 wt.%, Na_2O of 2.86–3.50 wt.%, and total alkalis ($K_2O + Na_2O$) of 8.34–8.92 wt.%, whereas low contents of TiO_2 of 0.20–0.26 wt.%. The values of $Mg^{\#}$ range from 22 to 33. The aluminum saturation index A/CNK is between 1.32 and 1.41, with an average value of 1.37, showing peraluminous characteristics (Fig. 6A; Supplementary Table 3). The high

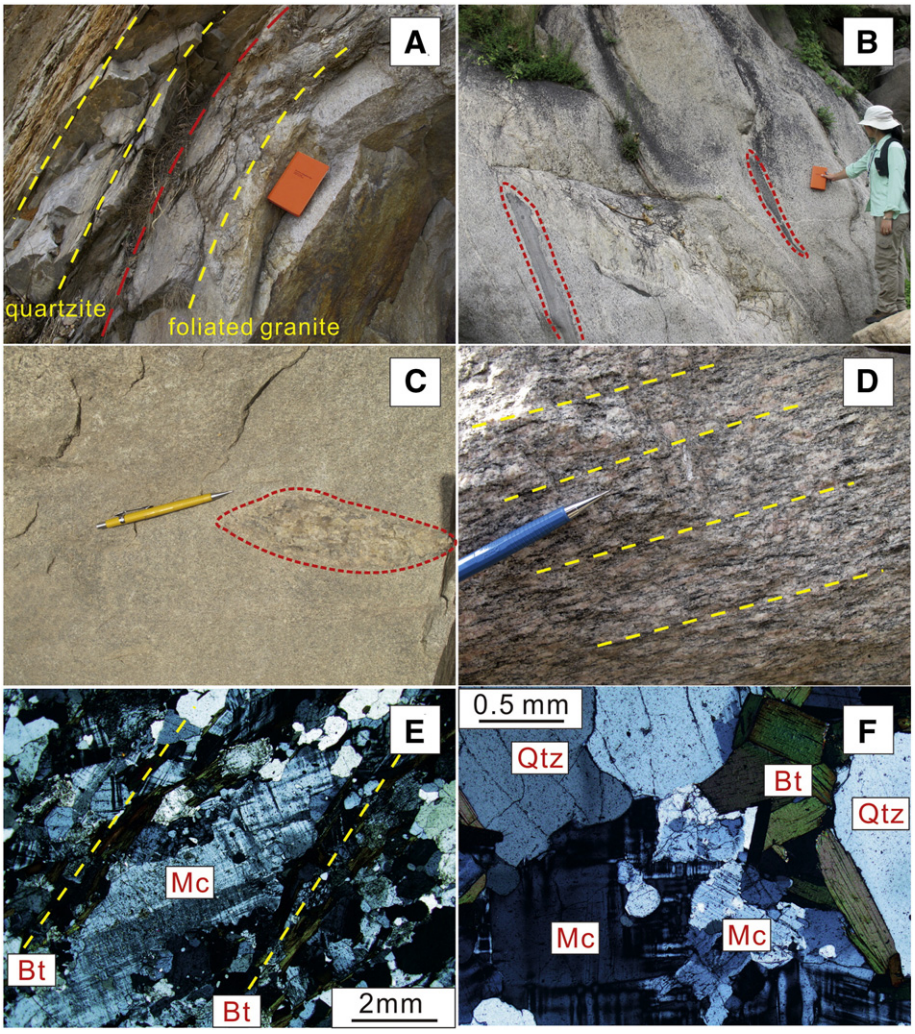

Fig. 4. Field photos and photomicrographs under microscope of the Wangjiazhuang granite in the Zanhuang mélange. A: Contact between foliated granite and Paleoproterozoic quartzite. The red dash line represents the contact margin and the yellow dash lines represent the foliation in the quartzite and foliated granite. B: Mafic inclusions in the Wangjiazhuang granite. C: Felsic inclusions in the Wangjiazhuang granite. D: Foliation in the Wangjiazhuang granite. E: Lineation defined by orientation of elongated biotite in the Wangjiazhuang granite. The yellow dash lines represent the orientation of the biotite. F: Granite containing microcline (Mc), quartz (Qtz) and biotite (Bt).

K_2O content of the Wangjiazhuang granite is comparable to that of the shoshonitic series on the K_2O vs. SiO_2 diagram (Fig. 6B).

The Wangjiazhuang granite has a large variation and enrichment in trace elements with 19.3–22 ppm Ga, 232–294 ppm Rb, 206–355 ppm Zr, 15.5–24.7 ppm Nb, 30.9–56.8 ppm Y (Supplementary Table 3). The total REEs contents of the Wangjiazhuang granite are high (Fig. 7; Supplementary Table 3), and show wide variations (ΣREE = 282.1–587.1 ppm, average value = 441.8 ppm) with very strong negative Eu anomalies ($Eu/Eu^* = 0.25–0.31$) (Fig. 7A). The Wangjiazhuang granite is highly enriched in LREEs ($(La/Sm)_N = 4.4–4.9$; $(La/Yb)_N = 8.5–31.4$) and has relatively flat HREE ($(Gd/Yb)_N = 1.3–3.3$) patterns (Fig. 7A). On the primitive mantle-normalized spidergram, the

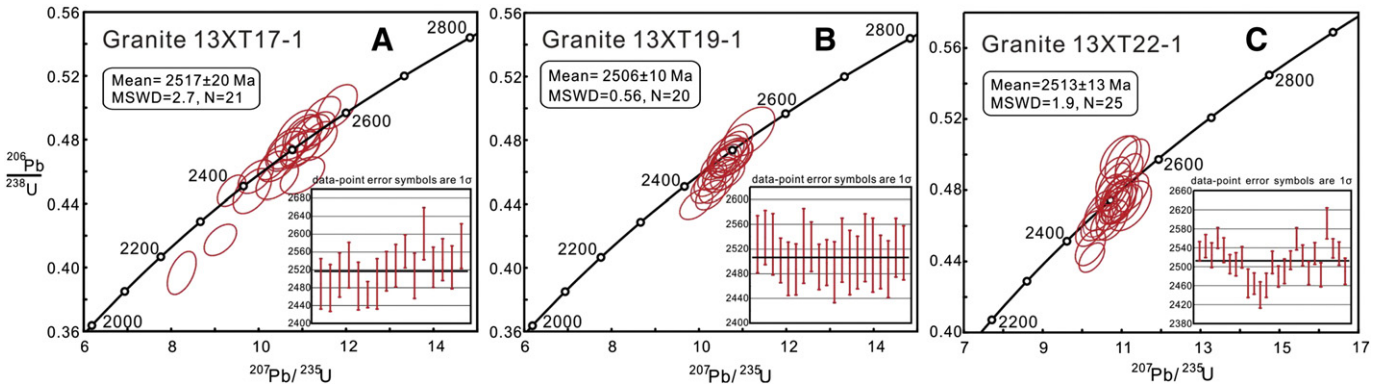

Fig. 5. Concordia of zircons from the Wangjiazhuang granite in the Neoarchean Zanhuang mélange.

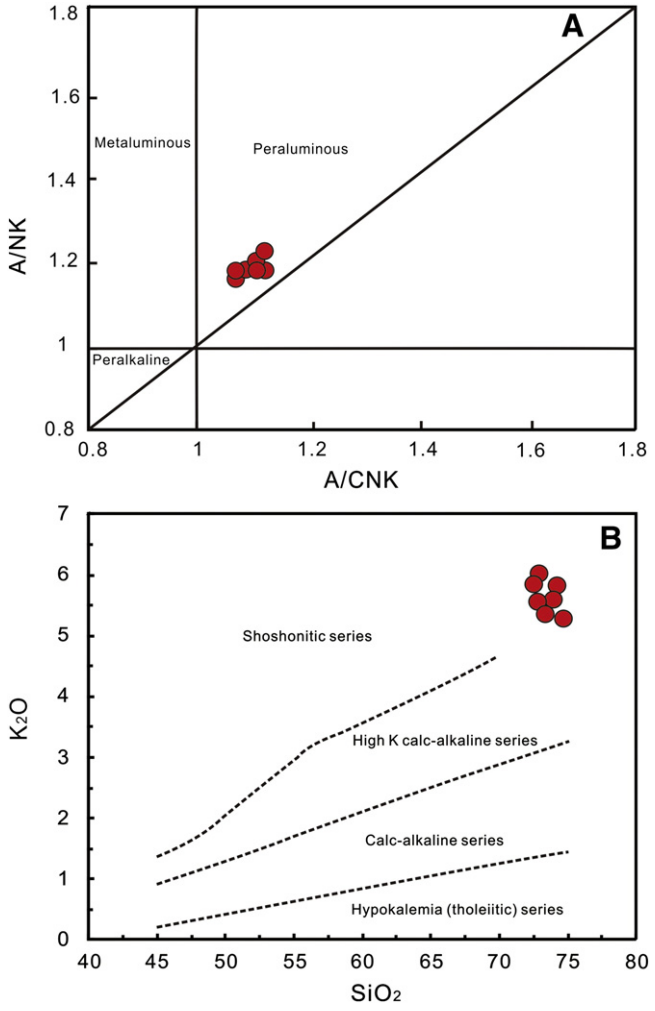

Fig. 6. A/NK vs. A/CN (A) and K_2O vs. SiO_2 (B) diagrams of the Wangjiazhuang granite in the Neoarchean Zanhuang mélange. A/NK = Al/(Na + K) (molar ratio). A/CNK = Al/(Ca + Na + K) (molar ratio).

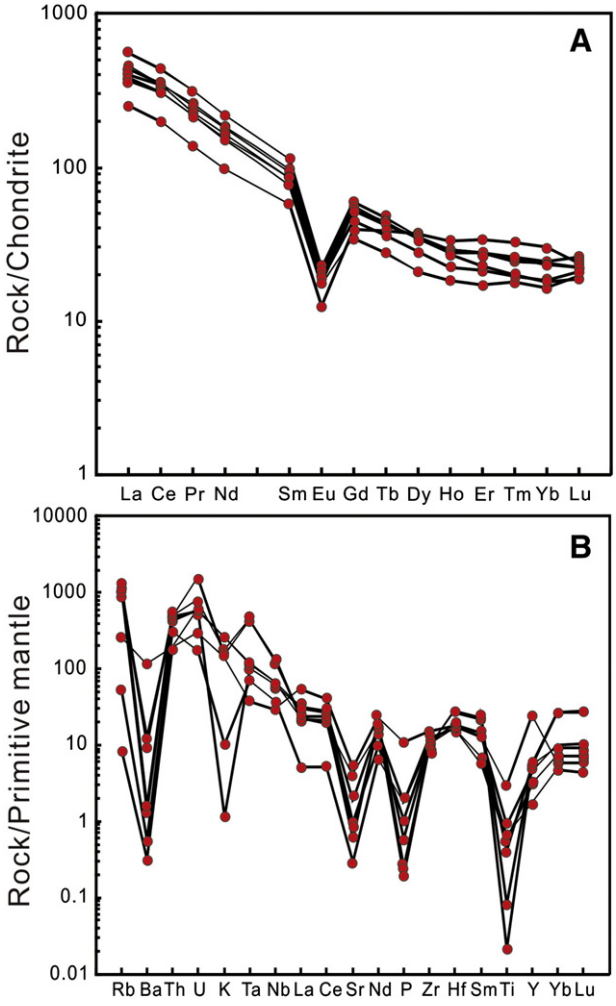

Fig. 7. Chondrite-normalized REE distribution patterns (A) and primitive mantle-normalized spidergrams (B) of the Wangjiazhuang granite in the Zanhuang mélange.

Wangjiazhuang granite has distinctly negative anomalies in Ba, Sr, P and Ti (Fig. 7B). The negative Ba, Sr and Eu anomalies might be associated with residue of plagioclase in the magma source, whereas the negative P anomalies should be attributed to the residue of apatite.

5.3. Sm–Nd isotopes

Samarium–Nd isotopic compositions of three samples from the Wangjiazhuang granite are given in Supplementary Table 4. The $^{143}Nd/^{144}Nd$ values are between 0.511162 and 0.511311. They have small positive initial εNd (t) values (+0.12–+1.13) (Supplementary Table 4) with one-stage Nd mantle-depletion model ages (T_{DM}) ranging from 2750 to 2863 Ma with a weighted average of 2799 Ma, while two-stage Nd mantle-depletion model ages (T_{DM2}) range from 2784 to 2869 Ma with a weighted average of 2821 Ma (Supplementary Table 4).

6. Discussion

6.1. Formation age of the Wangjiazhuang granite

All of the zircon grains from the three samples of the Wangjiazhuang granite are characterized by oscillatory zoning (Supplementary Fig. 1), variably high Th/U ratios (Supplementary Table 1), and fractionated REE patterns with strong negative Eu anomalies and slightly positive Ce anomalies (Supplementary Fig. 2), which are consistent with the characteristics of magmatic zircons (Corfu et al., 2003; Hoskin and Schaltegger, 2003; Rubatto, 2002; Wu and Zheng, 2004). Based on zircon CL images, trace element characteristics and $^{207}Pb/^{206}Pb$ ages, the weighted mean $^{207}Pb/^{206}Pb$ age of ca. 2.5 Ga of all the three samples are interpreted to represent the intrusion age of Wangjiazhuang granite.

6.2. Assessment of alteration and element mobility

Most Precambrian magmatic rocks, particularly Archean rocks, have been influenced by late metamorphism and deformation that change the original geochemical composition and magmatic textures (Middelburg et al., 1988; O'Neil et al., 2011; Ordóñez-Calderón et al., 2008; Panahi et al., 2000; Polat and Hofmann, 2003). There is at least one stage of later intrusions in the Central Orogenic Belts that occurred at ca. 2.1 Ga after the ca. 2.5 Ga magmatic event (Yang et al., 2011a,b). In addition, the Zanhuang massif underwent strong metamorphism and deformation at ca. 1.85 Ga which is widespread in the whole NCC (Deng et al., 2014; Kusky and Li, 2003; Kusky et al., 2011a; Peng et al., 2014; Wang et al., 2013a). Therefore, it is important to assess the influence from the late metamorphism and deformation on the mobility of the major and trace elements and isotopic elements for the Wangjiazhuang granite.

All the samples are least weathered and altered (Fig. 4). Very few zircons with thin metamorphic rims can be observed from the CL images of all the zircons (Supplementary Fig. 1) indicating low-impacts from later regional metamorphism and deformation. The minor loss on ignition

(LOI) values (less than 1 wt.%) and narrow Ce/Ce* ratios ranging from 1.01 to 1.14 suggest that the hydration is very weak during late alteration (Supplementary Table 3; Polat and Hofmann, 2003). The distribution patterns are consistent with each other on the chondrite- and primitive mantle-normalized diagrams demonstrating that the REE and HSFE are relatively immobile (Fig. 7). Thus, the geochemistry data presented in this paper can be used to interpret the petrogenesis of the Wangjiazhuang granite.

6.3. Petrogenesis of the Wangjiazhuang granite

6.3.1. An A-type affinity of the Wangjiazhuang granite

The term "A-type" granite was first proposed by Loiselle and Wones (1979) to define alkaline, anhydrous anorogenic granite. Many studies have shown that the composition of A-type granites are diverse, varying from quartz syenites to peralkaline granites (Eby, 1990; Kemp and Hawkesworth, 2003; King et al., 1997; Zhang et al., 2007a,b). However, compared to alkaline granitoids, low Sr and CaO contents, high SiO_2, $Na_2O + K_2O$ and REE contents, and high K_2O/Na_2O and Ga/Al ratios have been defined for A-type granite (Collins et al., 1982; Eby, 1990; Yang et al., 2006; Zhang et al., 2007a,b).

The Wangjiazhuang granite is characterized by their relatively high alkali contents and low CaO contents (SiO_2 = 72.6–74.6 wt.%; $Na_2O + K_2O$ = 8.34–8.92 wt.%, CaO = 0.53–1.16 wt.%) which are consistent with those of classic A-type granites (SiO_2 = 70 wt.%: $Na_2O + K_2O$ = 7–11 wt.% and CaO < 1.8 wt.%) (Eby, 1990). It shows enrichment of Nb (15.5–24.7 ppm), Ga (19.3–22 ppm) and Y (30.9–56.8 ppm), which are similar to the characteristics of typical A-type granites (Collins et al., 1982; Eby, 1990, 1992; Whalen et al., 1987). The 10,000 Ga/Al ratios vary from 2.69 to 3.05 with an average of 2.90, which is slightly lower than the global average of 3.75 for A-type granites (Whalen et al., 1987), but similar to those of aluminous A-type granites with much younger ages from northern China (Wu et al., 2002). The REE contents (282.1–587.1 ppm) are similar to granitoids that have been classified as A-type granitoids listed in Eby (1990). In the classification diagram of Na_2O vs. K_2O, ($K_2O + Na_2O$) vs. 10,000 Ga/Al and ($K_2O + MgO$) vs. 10,000 Ga/Al, they all plot in the field of A-type granite (Fig. 8; Whalen et al., 1987).

Generally, A-type granites have a relatively high temperature origin, which is different from other types of granite. The saturation temperature of zircons can generally be considered to approximately represent the initial magma temperature of granitic rocks (King et al., 2001; Miller et al., 2003; Watson and Harrison, 1983). Hydrothermal experiments in the temperature range 750–1020 °C have defined the saturation behavior of zircon in crustal anatectic melts as a function of both temperature and composition. The results provide a model of zircon solubility given by:

$$\ln D_{Zr}^{zircon/melt} = (-3.80 - [0.85(M-1)]) + 12900/T$$

where $D_{Zr}^{zircon/melt}$ is the concentration ratio of Zr in the zircon to that in the melt, T is the absolute temperature, and M is the cation ratio $(Na + K + 2Ca)/(Al - Si)$ (Watson and Harrison, 1983). The saturation temperature of zircons from the Wangjiazhuang granite is between 806 and 861 °C (Supplementary Table 3) with an average value of 836 °C, which is interpreted to represent the formation temperature of the Wangjiazhuang granite (Watson and Harrison, 1983). This temperature is higher than typical I-type granites but similar to those of typical A-type granites worldwide (Bonin, 2007; Clemens et al., 1986; King et al., 1997, 2001; Miller et al., 2003; Zhao et al., 2008).

In conclusion, it is suggested that the Wangjiazhuang granite in the Neoarchean Zanhuang tectonic mélange belt shows a typical affinity of A-type granites.

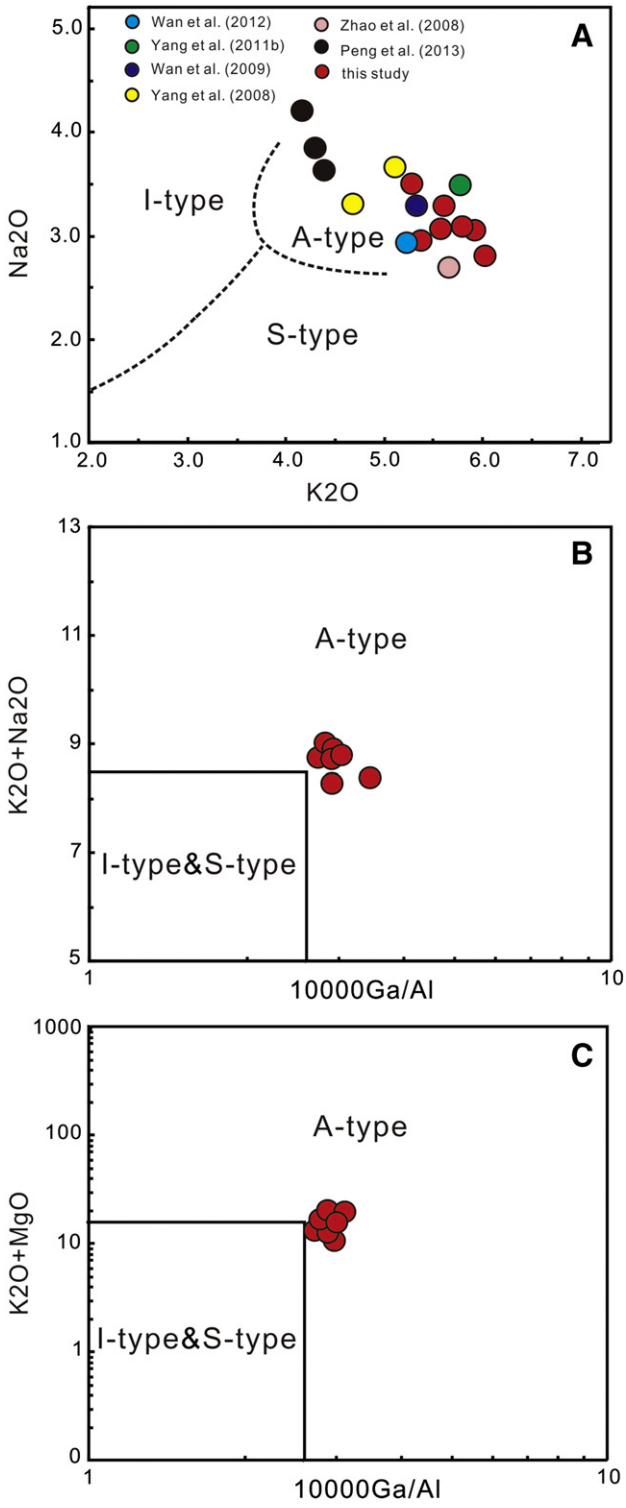

Fig. 8. Na_2O vs. K_2O (A), ($K_2O + Na_2O$) vs. 10,000 Ga/A1 (B), and ($K_2O + MgO$) vs. 10,000 Ga/A1 (C) diagrams of the Wangjiazhuang granite in the Neoarchean Zanhuang mélange (after Whalen et al., 1987).

6.3.2. Magma source nature

The genesis of A-type granite is controversial, with two categories including crustal and mantle regions suggested as their source. The high contents of Si, K, and Rb/Sr ratios (1.80 to 3.21, average value = 2.54), low contents of Mg and Cr (Supplementary Table 3) suggest that the Wangjiazhuang granite can't be derived from mantle-derived

melts. The low ε_{Nd} (t) values (+0.12 to +1.13) (Supplementary Table 4) of the Wangjiazhuang granite are also consistent with contamination by ancient crust. Based on a crustal origin, two models have been proposed to account for the nature of the crustal source: 1) partial melting of a dry and granulitic residue from extraction of prior granitic melt (Clemens et al., 1986; Collins et al., 1982; Whalen et al., 1987) and 2) remelting of tonalite or granodiorite at high temperature (Creaser et al., 1991; Patiño Douce, 1997; Skjerlie and Johnston, 1993). Experiments show that remelting of refractory granulitic residues generated from partial melting of crustal rocks depletes alkalis relative to Al_2O_3 and TiO_2 relative to MgO (Patiño Douce and Beard, 1995), which is not consistent with the high $(Na_2O + K_2O)/Al_2O_3$ and TiO_2/MgO ratios of the Wangjiazhuang granite (Supplementary Table 3). For this reason, the first model is discounted.

Patiño Douce (1997) documented that dehydration melting of tonalite or granodiorite with plagioclase-rich residuum at high temperatures is capable of generating aluminous A-type granite. The Wangjiazhuang granite has peraluminous features (Fig. 6A). The obviously negative Sr and Eu anomalies suggest that plagioclase may have been preserved in the residue. Archean TTG gneisses with a dominance of tonalite are widespread in the Zanhuang massif (Wang et al., 2013a; Yang et al., 2013), which can provide a probable source for the Wangjiazhuang granite. In addition, the one stage Nd isotope model ages (2750–2863 Ma, average value = 2799 Ma) are older than the formation age of the Wangjiazhuang granite (ca. 2.5 Ga) and similar to the age of the TTG gneisses (ca. 2.7 Ga), suggesting that the Wangjiazhuang granite may have resulted from partial melting of the ca. 2.7 Ga TTG gneisses in the Zanhuang massif.

6.4. Overview of the ca. 2.5 Ga magmatic event in the NCC

The ca. 2.5 Ga magmatic event of granitic intrusions with similar geochemistry and petrogenesis is not just distributed in the Zanhuang massif (Fig. 1B-1), but is dispersed in the Central Orogenic Belt and Eastern Block of the NCC (Fig. 1B). The summary of reported ca. 2.5 Ga magmatic rocks with GPS coordinates is shown in Table 1 and location of every granitic pluton of this type is shown in Fig. 1B.

The ca. 2.5 Ga granitic rocks in the Central Orogenic Belt of the NCC mainly include granite, pegmatite, granitoid and monzogranite. Undeformed pegmatites have been reported from the Zanhuang massif (labeled as 1 in Fig. 1B) yielding $^{207}Pb/^{206}Pb$ ages of 2539 ± 44 Ma (Wang et al., 2013a) and 2504 ± 16 Ma (Deng et al., 2014) from magmatic zircons. Based on field observations, both the Wangjiazhuang granite (Fig. 1B) and pegmatite in the Zanhuang massif crosscut the fabrics and many sections of the Zanhuang mélange and have coeval ages of ca. 2.5 Ga. We therefore suggest that they formed in the same tectonomagmatic event (Wang et al., 2013a). SHRIMP dating of magmatic zircons from the Jiandeng potassic granite (Fig. 1B) in the Zanhuang massif yielded an age of 2490 ± 13 Ma (Table 1; Yang et al., 2011b). The geochemical characteristics show A-type affinity on a Na_2O vs. K_2O diagram (Fig. 8A). LA–ICPMS dating of magmatic zircons from the Haozhuang granite (Fig. 1B) in the Western Zanhuang Domain yielded $^{207}Pb/^{206}Pb$ ages of 2475–2509 Ma (Table 1; Fu et al., in preparation). On the Na_2O vs. K_2O classification diagram, they all plot in the A-type field (Fig. 8A). In the Wutai Complex (labeled as 2 in Fig. 1B), ca. 2517–2566 Ma magmatism has been reported in several places (Table 1; Liu et al., 1985; Wilde et al., 1997, 2005). Wilde et al. (2005) interpreted these relatively evolved granitoids to be derived from older basement consisting of TTG rocks of the NCC and are a consequence of subduction and related arc magmatism. In addition, formation ages of 2560 ± 6 Ma and 2520 ± 30 Ma from the Lanzhishan and Ekou granites (Fig. 1B) have been documented in the Wutai Complex which are also interpreted to be generated from older TTG rocks of the NCC basement (Liu et al., 1985). In the Fuping Complex (labeled as 3 in Fig. 1B), Li et al. (2004) reported ca. 2.5 Ga magmatic ages (Table 1) from zircon cores of potassic pegmatites and granite with low Th/U ratios and suggested that these granitic intrusions are related to a subduction event. Zhao et al. (2002) also described a pegmatite which yielded an igneous age of 2507 ± 11 Ma, interpreted to be a product of a magmatic arc system (Table 1). In the Huai'an Complex (labeled as 4 in Fig. 1B), Zhang et al. (2011) demonstrated that the Xuanhua and Manjinggou potassic granites (Fig. 1B) have igneous zircon ages of 2437–2493 Ma (Table 1) and suggested that they were formed by partial melting of lower crust. In the Dengfeng Complex (labeled as 5 in Fig. 1B), Wan et al. (2009) reported a formation age of 2513 ± 33 Ma from the Lujiagou monzogranite (Fig. 1B) with geochemical characteristics of A-type granites (Table 1) and suggested that the monzogranite is a product of magmatism after an earlier collision.

For the Eastern Block of the NCC, the ca. 2.5 Ga granitic rocks mainly include tonalite, monzogranite, granodiorite, syenogranite and potassic granite. In the Eastern Hebei Province (labeled as 5 in Fig. 1B), Geng et al. (2006) reported widely distributed tonalites which yield an intrusion age of 2550 ± 2 Ma (Table 1), and demonstrated that the formation of such a great amount of magma was a critical crustal generation stage at the end of the Neoarchean. Magmatic zircons from two monzogranite samples yield $^{207}Pb/^{206}Pb$ intrusion ages of 2512 ± 12 Ma and 2525 ± 10 Ma (Table 1; Nutman et al., 2011) and interpreted the monzogranite to have been formed during magmatic arc evolution. These monzogranites show marked negative Ti anomalies and enrichment of the light REE relative to the heavy REE (Nutman et al., 2011), which are similar to those of the Wangjiazhuang granite. The Qinhuangdao potassic granites (Fig. 1B) with A-type affinity (Fig. 8A) were reported to have $^{207}Pb/^{206}Pb$ formation ages of 2522–2523 Ma and were suggested to have resulted from the melting of ancient crust (Yang et al., 2008). Wan et al. (2012) also reported that the Qinhuangdao granite (Fig. 1B) has a $^{207}Pb/^{206}Pb$ formation age of 2511 ± 10 Ma (Table 1) and suggested that it was formed through melting of continental crust and its formation marks a tectono-magmatic event at the end of the Neoarchean. This sample falls into the A-type granite field in the Na_2O vs. K_2O diagram (Fig. 8A). In Western Liaoning Province (labeled as 7 in Fig. 1B), Kröner et al. (1998) reported that intrusion of granitoids in the Jianping Complex (Fig. 1B) began at 2521.8 ± 0.8 Ma (Table 1) and speculated that the Jianping Complex was part of an active continental margin in the Neoarchean. In Western Shandong Province (labeled as 8 in Fig. 1B), Wan et al. (2010) reported SHRIMP U–Pb zircon ages of 2490–2539 Ma (Table 1) from magmatic rocks and suggested that these Neoarchean magmatic rocks were probably formed in an arc environment. Zhao et al. (2008) also reported potassic granites with A-type affinity with SHRIMP U–Pb zircon igneous age of 2530 ± 7 Ma. Peng et al. (2013) described late Neoarchean Taishan potassic granites (Fig. 1B) which yielded ages of 2517 ± 21 Ma, 2526 ± 38 Ma and 2462 ± 18 Ma (Table 1) and suggested that they formed in an active subduction regime in a continental crustal evolution process. The geochemical results plot into the field of A-type granite (Fig. 8A).

In conclusion, it is clear that the strong ca. 2.5 Ga magmatic event with the prominent characteristics of emplacement of the ca. 2.5 Ga granitic rocks is widely distributed in the Central Orogenic Belt and Eastern Block of the NCC. Based on the above information, these granitic rocks with concentrated magmatic zircon ages of ca. 2.5 Ga have similar geochemical characteristics and probably formed in a similar tectonic setting. Their geochemical characteristics show A-type granite affinity with relatively high potassium contents (Peng et al., 2013; Yang et al., 2011b; Zhang et al., 2011; Zhao et al., 2008). The most accepted idea on the petrogenesis of the ca. 2.5 Ga granitic rocks is that these granitic rocks formed from partial melting of the older TTG lower crust in an arc setting associated with subduction (Deng at al., 2014; Huang et al., 2010; Kröner et al., 1998; Li et al., 2006; Liu et al., 1985, 1990; Nutman et al., 2011; Peng et al., 2013; Trap et al., 2009; Wan et al., 2009, 2010, 2012; Wang et al., 2013a; Wilde et al., 1997, 2005; Yang et al., 2011b; Zhang et al., 2011; Zhao et al., 2002, 2005, 2008; Zhou et al., 2011), though some people argue that they were related to the underplating by a mantle plume (Lu et al., 2008; Wu et al., 2012; Zhao and Guo,

Table 1
Summary of magmatic zircon ages (Ca. 2500 Ma) from granitic rocks in the whole North China Craton.

Location	GPS location	Lithology	Sample	Formation age (Ma)	Method	Reference	Geochemistry	
							Na_2O	K_2O
Central Orogenic Belt								
Zanhuang Massif (ZH)								
Wangjiazhuang	N 37°19′37.2″, E 114°11′19.6″	A-type granite	168-1	2540 ± 23	LAICPMS	Wang et al. (2013a)		
Wangjiazhuang	N 37°18′2.2″, E 114°13′29.9″	A-type granite	91-1b	2493 ± 22	LAICPMS	Wang et al. (2013a)		
Wangjiazhuang	N 37°19′36.7″, E 114°11′30.4″	A-type granite	13XT17-1	2517 ± 20	LAICPMS	this study		
Wangjiazhuang	N 37°19′37″, E 114°11′19.5″	A-type granite	13XT19-1	2506.4 ± 9.8	LAICPMS	this study		
Wangjiazhuang	N 37°18′1.1″, E 114°13′30.1″	A-type granite	13XT22-1	2513 ± 13	LAICPMS	this study		
Lujiazhuang	N 37°13′13.8″, E 114°06′22.1″	Pegmatite	76-5c	2539 ± 44	LAICPMS	Wang et al. (2013a)		
Lujiazhuang	N 37°13′06″, E 114°06′05″	Pegmatite	13XT10-2	2504 ± 16	LAICPMS	Deng et al. (2014)		
Jiandeng	N 37°29′08″, E 114°19′30.4″	Potassic granite	Z03-3	2490 ± 13	SHRIMP	Yang et al. (2011b)	3.49	5.76
Haozhuang	N 37°29′22.4″, E 114°12′36.4″	Granite	13XTA-31-1	2475 ± 37	LAICPMS	Fu et al., in prep.	6.45	3.35
Haozhuang	N 37°29′22.6″, E 114°12′36.2″	Granite	13XTA-31-2	2509 ± 24	LAICPMS	Fu et al., in prep.	6.52	4.2
Wutai Complex (WT)								
Lanzhishan		Granite	PC-95-94	2553 ± 8	SHRIMP	Wilde et al. (1997)		
Lanzhishan		Granite	PC-95-96	2537 ± 10	SHRIMP	Wilde et al. (1997)		
Ekou		Granite	95-19	2555 ± 6	SHRIMP	Wilde et al. (1997)		
Ekou		Granite	PC-95-34	2566 ± 13	SHRIMP	Wilde et al. (1997)		
Longquanguan		Granitoid	WL9	2540 ± 18	SHRIMP	Wilde et al. (1997)		
Longquanguan		Granitoid	WN11	2541 ± 4	SHRIMP	Wilde et al. (1997)		
Longquanguan		Granitoid	WL12	2543 ± 7	SHRIMP	Wilde et al. (1997)		
Lanzhishan		Granite	Ag5-5	2560 ± 6	SGD	Liu et al. (1985)		
Ekou		Granite	Ea-r	2520 ± 30	SGD	Liu et al. (1985)		
Guangmingsi		Granite	Ag6-2	2522 ± 17	SGD	Liu et al. (1985)		
Guangmingsi	N 39°02′26″, E 113°37′09″	Granitoid	95-PC-76	2531 ± 5	SHRIMP	Wilde et al. (2005)		
Shifo	N 38°55′39″, E 113°38′33″	Granitoid	95-PC-98	2531 ± 4	SHRIMP	Wilde et al. (2005)		
Chechang–Beitai	N 39°05′32″, E 113°38′14″	Granitoid	WC5	2538 ± 6	SHRIMP	Wilde et al. (2005)		
Chechang–Beitai	N 39°05′14″, E 113°38′31″	Granitoid	WC6	2546 ± 6	SHRIMP	Wilde et al. (2005)		
Chechang–Beitai	N 39°12′22″, E 113°42′56″	Granitoid	WC7	2552 ± 11	SHRIMP	Wilde et al. (2005)		
Chechang–Beitai	N 39°04′31″, E 113°39′53″	Granitoid	95-PC-6B	2551 ± 5	SHRIMP	Wilde et al. (2005)		
Wangjiahui	N 39°01′06″, E 113°01′01″	Granitoid	95-PC-62	2520 ± 9	SHRIMP	Wilde et al. (2005)		
Wangjiahui	N 39°01′00″, E 113°01′04″	Granitoid	95-PC-63	2517 ± 12	SHRIMP	Wilde et al. (2005)		
Fuping Complex (FP)								
Xinzhuang		Pegmatite	FP224	2507 ± 11	SHRIMP	Zhao et al. (2002)		
Banqiaogou		Pegmatite	F01101-2	~2500	SHRIMP	Li et al. (2004)		
Banqiaogou		Anatetic granite	F01101-1	~2500	SHRIMP	Li et al. (2004)		
Huai'an Complex (HA)								
Xuanhua	N 40°41′45″, E 115°12′28″	Potassic granite	XGY01-2	2493 ± 6	SHRIMP	Zhang et al. (2011)		
Manjinggou	N 40°20′09″, E 114°27′29″	Biotite granite	DJG12	2437 ± 10	LAICPMS	Zhang et al. (2011)		
Dengfeng Complex (DF)								
Lujiagou	N 34°27′54″, E 112°48′14″	Monzogranite	XS0416-11	2513 ± 33	SHRIMP	Wan et al. (2009)	3.33	5.41
Eastern Block								
Eastern Hebei Province (EH)								
Yuhuzhai		Tonalite	TP22	2550 ± 2	SHRIMP	Geng et al. (2006)		
Beidaihe	N 39°48′40″, E 119°29′05″	Monzogranite	J08/12	2512 ± 12	SHRIMP	Nutman et al. (2011)		
Beidaihe	N 39°48′47″, E 119°29′31″	Monzogranite	J08/16	2525 ± 10	SHRIMP	Nutman et al. (2011)		
Qinhuangdao		Granite	FW04-54	2523 ± 6	LAICPMS	Yang et al. (2008)	3.67	5.07
Qinhuangdao		Granodiorite	FW04-42	2522 ± 5	LAICPMS	Yang et al. (2008)	3.28	4.68
Qinhuangdao		Syenogranite	J0817	2511 ± 10	SHRIMP	Wan et al. (2012)	2.94	5.27
Western Liaoning Province (WL)								
Jianping		Granitoid		2521.8 ± 0.8	SGD	Kroner et al. (1998)		
Western Shandong Province (WS)								
Lushan	N 36°19′09″, E 118°11′19″	Syenogranite	S0788	2525 ± 13	SHRIMP	Wan et al. (2010)		
Shihaishan	N 35°20′39″, E 117°32′46″	Syenogranite	S0516	2533 ± 8	SHRIMP	Wan et al. (2010)		
Tianhuang	N 35°23′59″, E 117°07′23″	Granodiorite	S0705	2525 ± 8	SHRIMP	Wan et al. (2010)		
Feicheng	N 36°23′59″, E 116°46′22″	Monzogranite	S0827	2503 ± 11	SHRIMP	Wan et al. (2010)		
Sishui	N 35°46′34″, E 117°08′37″	Monzogranite	S0777	2513 ± 12	SHRIMP	Wan et al. (2010)		
Guimengding	N 35°33′22″, E 117°57′29″	Monzogranite	S0717	2534 ± 8	SHRIMP	Wan et al. (2010)		
Guimengding	N 35°33′30″, E 117°50′39″	Monzogranite	S0710	2515 ± 12	SHRIMP	Wan et al. (2010)		
Taishan	N 35°33′42″, E 117°50′42″	Monzogranite	S0711	2539 ± 15	SHRIMP	Wan et al. (2010)		
Taishan	N 36°16′21″, E 117°02′14″	Monzogranite	SY0333	2507 ± 27	SHRIMP	Wan et al. (2010)		
Yanlingguan	N 36°02′14″, E 117°34′46″	Monzogranite	SY0310	2501 ± 15	SHRIMP	Wan et al. (2010)		
Qixingtai	N 36°27′45″, E 117°23′06″	Monzogranite	S0727	2508 ± 10	SHRIMP	Wan et al. (2010)		
Qixingtai	N 36°28′49″, E 117°23′10″	Monzogranite	S0728	2518 ± 9	SHRIMP	Wan et al. (2010)		
Lushan	N 36°17′21″, E 118°03′20″	Monzogranite	S0791	2508 ± 20	SHRIMP	Wan et al. (2010)		
Mengyin	N 35°46′28″, E 118°11′19″	Syenogranite	S0508	2531 ± 8	SHRIMP	Wan et al. (2010)		
Lushan	N 36°17′19″, E 118°03′17″	Syenogranite	S0789	2517 ± 13	SHRIMP	Wan et al. (2010)		
Lushan	N 36°19′09″, E 118°11′19″	Syenogranite	S0788	2525 ± 13	SHRIMP	Wan et al. (2010)		
Yishan	N 36°12′19″, E 118°37′48″	Syenogranite	S0787	2490 ± 10	SHRIMP	Wan et al. (2010)		
Yinglingshan		Potassic granite	YS06-30	2530 ± 7	SHRIMP	Zhao et al. (2008)	2.67	5.68
Taishan	N 35°27′29″, E 118°05′53″	Potassic granite	08YS-105	2517 ± 21	LAICPMS	Peng et al. (2013)	4.26	4.11
Taishan	N 35°28′40″, E 118°03′18″	Potassic granite	08YS-112	2526 ± 38	LAICPMS	Peng et al. (2013)	3.60	4.44
Taishan	N 35°21′42″, E 117°26′48″	Potassic granite	08YS-142	2462 ± 18	LAICPMS	Peng et al. (2013)	3.74	4.33

Note: Zircon U–Pb: LAICPMS: laser ablation inductively coupled plasma mass spectrometry; SHRIMP: sensitive high resolution ion microprobe; SGD: single grain dissolution method by Krogh, 1973. Major element values are in wt.%.

2012; Zhao et al., 2012). It is noteworthy that the ca. 2.5 Ga granitic rocks with similar geochemistry and tectonic setting seem to be only exposed in the Central Orogenic Belt and the Eastern Block of the NCC. There are ca. 2.5 Ga granitic rocks distributed in the Western Block, but they have different geochemical characteristics and reflect a different tectonic setting (Jian et al., 2012).

6.5. Geodynamic implication for the NCC

6.5.1. Arc–continent collision at ca. 2.5 Ga in the NCC

Although the collisional mechanism of the NCC has been controversial for several decades, more evidence shows that the first collision between the Fuping arc and Eastern Block attributed to arc–continent collision over a west-dipping subduction zone (Kusky, 2011a, 2011b; Kusky and Li, 2003). Recently, we documented a Neoarchean tectonic mélange and a suite of passive margin sediments grading up into a foreland basin sequence (Wang et al., 2013a), separating TTG gneisses of the Western Zanhuang Domain (Fuping arc) with SHRIMP zircon U–Pb age of ca. 2692 ± 12 Ma (Trap et al., 2009) and TTG gneisses of Eastern Block (continental block) with late Archean ages (Kusky and Li, 2003). The petrology, geochemical and geochronological analyses on the late mafic dikes that crosscut all the units of the mélange also suggest that the first collision in the NCC was an arc–continent collision at ca. 2.5 Ga (Deng et al., 2013, 2014). We therefore suggest that the Fuping arc and the Eastern Block continent collided prior to 2.5 Ga during arc–continent collision (Wang et al., 2013a).

6.5.2. Reversed subduction polarity event after arc–continent collision in the NCC

The whole Neoarchean Zanhuang mélange was intruded by a suite of 2.53 Ga mafic dike swarms (Deng et al., 2014). Based on field and structural studies on the Neoarchean Zanhuang mélange, geochemical, geochronological and isotopic studies on the mafic dikes in the Zanhuang massif of the Central Orogenic Belt, and comparative analyses with coeval mafic dikes in the NCC (Li et al., 2010; Liu et al., 2014; Tang et al., 2007; Wu et al., 2014), we propose that the Neoarchean mafic dikes in the Central Orogenic Belt and Eastern Block of the NCC form a large regional mafic dike swarm in the NCC (Deng et al.., 2013, 2014; Wang et al., 2013a). These mafic dikes were generated from the melting of an enriched mantle that provided parental magma for the mafic dike swarms (Fig. 9; Deng et al., 2013, 2014). Deng et al. (2014) suggest that the mantle source of 2.53 Ga mafic dike swarms was related to an arc and enriched by a subduction-related event. In addition, the hornblendites in the Neoarchean Zanhuang mélange are considered to be related to arc or subduction-related environment (Deng et al., 2014; Polat et al., 2012). We proposed that a new east-dipping subduction zone developed below the western side of the newly sutured active island arc/Eastern Block. The new subduction resulted in the lithospheric mantle becoming enriched by the new subduction slab-derived melts and fluids, and gave rise to the formation of 2.53 Ga mafic dikes. Meanwhile, the rising parental magma of these mafic dike swarms induced partial melting of the old and thickened TTG crust leading to the formation of the ca. 2.5 Ga A-type Wangjiazhuang granite in the Zanhuang massif and its correlatives throughout the eastern NCC (Deng et al., 2014; Wang et al., 2013a). In this study, we further proposed that the ca. 2.5 Ga potassic granitic rocks are distributed both in the Central Orogenic Belt and the Eastern Block of the NCC and are contemporaneous with the intrusion of the 2.5 Ga mafic dike swarms in the NCC, and suggest that these ca. 2.5 Ga magmatic rocks in the NCC were formed through partial melting of the older thickened arc (Fuping arc) and older TTG gneisses (Fig. 9; Deng et al., 2014; Wang et al., 2013a).

Based on geochemical and geochronological studies on the ca. 2.5 Ga mafic dike swarms and the granitic rocks in the Zanhuang massif of the NCC, and a comparison study with similar-aged mafic dike swarms and granitic rocks in the Central Orogenic Belt and Eastern Block of the NCC (Deng et al., 2013, 2014; Wang et al., 2013a and this study), we propose a Neoarchean subduction polarity reversal event that initiated subduction dipping to the east following the arc–continent collision between the Eastern Block and the Fuping arc to explain the intrusion of the 2.5 Ga mafic dike swarms and the ca. 2.5 Ga granitic rocks in the Central Orogenic Belt and Eastern Block. We suggest that this subduction reversal event occurred beneath the western margin of the arc–continent collision zone. The enriched mantle starts to melt after the subduction reversal event and resulted in the development of the mafic dike swarms. The rising magma that is parentally from melting of the enriched mantle ponded at the bottom of the old and thickened lower crust with arc affinity and gave rise to its melting and then produced the ca. 2.5 Ga granitic rocks in the Central Orogenic Belt and Eastern Block of the NCC (Fig. 9).

6.5.3. Subduction polarity reversal events worldwide

The Neoarchean subduction reversal event after an earlier arc–continent collision in the NCC can be compared to many examples worldwide. McKenzie (1969) proposed that the subduction direction beneath an island arc will reverse following arc–continent collision. Seismic tomography and physical modeling evidence for subduction polarity reversal has been shown in the Solomon island arc (Copper and Taylor, 1985), Taiwan (Chemenda et al., 1997) and the Alpine and the Apennine belts (Vignaroli et al., 2008). Although geophysical evidence can effectively show modern subduction polarity, geological

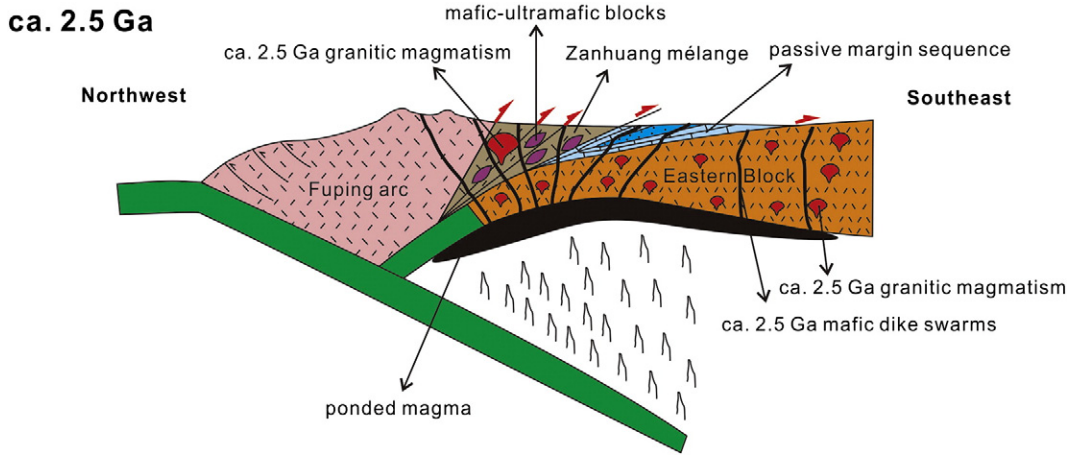

Fig. 9. Model of interpreted geodynamic origin of the ca. 2.5 Ga magmatic event in the Central Orogenic Belt of the NCC. A new east-dipping reversed subduction happened at 2.5 Ga, following the collision between the Eastern Block of the NCC and the intra-oceanic arc terrane to the west. This east-subduction polarity reversal event results in the melting of the enriched mantle, and then gives rise to the formation of the ca. 2.5 Ga Wangjiazhuang granite.

and structural data can also show convincing evidence for the direction of the subduction polarity in ancient orogens. Based on field and structural data of the thrust emplacement of the Hispaniola peridotite belt, Draper et al. (1996) proposed an arc polarity reversal in the mid-Cretaceous Caribbean. According to the geodynamic model based on structural and geological data for southern Kamchatka, Konstantinovskaia (2001) proposed a subduction polarity reversal, which is the most characteristic feature following arc–continent collision. All the above examples show that the subduction polarity reversal events are well-documented in Cenozoic and Mesozoic orogens worldwide. However, they have been rarely reported from Archean orogens. In this paper, we propose a Neoarchean subduction polarity reversal beneath the Fuping arc following arc–continent collision. Teng et al. (2000) suggested that the subduction polarity reversal in northern Taiwan beneath the Taiwan orogen was caused by the breakoff of the Eurasian slab, which created a mantle window for the lateral movement of the Philippine Sea plate. In addition, Clift et al. (2003) proposed that the subsequent subduction polarity reversal was due to the continuous tearing and retreat of the oceanic lithosphere, which provided space for the subduction polarity reversal of the new oceanic plate. Condie and Kröner (2013) suggested that oceanic arcs in the Archean were thicker than in younger geological times due to the higher degrees of melting in the mantle and the more buoyant oceanic lithosphere, and might have had a higher tendency to accrete to each other. We propose that the arc–continent collision between the Eastern Block continent and the Fuping arc was the initial trigger for the subsequent subduction polarity reversal. The arc–continent collision made the western margin of the accreted active arc–Eastern Block continent become a more vulnerable place where the new subduction was initiated with polarity reversal to the east. This change in subduction polarity leads to the formation of ca. 2.5 Ga mafic dikes and granitic rocks in the Central Orogenic Belt and Eastern Block of the NCC (Fig. 9).

7. Conclusions

The following conclusions are drawn from this study:

1) Geochemical data shows that the Wangjiazhuang granite has peraluminous and potassic characteristics and belongs to the shoshonitic series. They geochemically fall into the A-type granite field.
2) New LA–ICP–MS zircon $^{207}Pb/^{206}Pb$ ages of the Wangjiazhuang granite confirm that it is ca. 2.5 Ga in age. Combined with previous studies on the ca. 2.5 Ga magmatic rocks in the Central Orogenic Belt and Eastern Block in the NCC, we propose that the ca. 2.5 Ga magmatic event in the Zanhuang massif is widely distributed in the North China Craton, implying that these A-type plutonic rocks formed in a similar tectonic setting related to subduction.
3) A Neoarchean subduction polarity reversal event following the 2.5 Ga collision of the eastern NCC with an arc is proposed to account for the intrusion of the 2.5 Ga granitic plutons in the Central Orogenic Belt and Eastern Block of the NCC. This Neoarchean subduction polarity reversal event is similar to those in younger geological times and provides strong evidence that plate tectonics was operating by the end of the Nearchean.
4) The subduction polarity reversal event at ca. 2.5 Ga in the NCC resulted in the melting of the enriched mantle. Meanwhile, the rising magma induced partial melting of old and thickened TTG lower crust leading to the formation of the ca. 2.5 Ga granitic rocks including the ca. 2.5 Ga Wangjiazhuang granite which intrudes the Neoarchean Zanhuang tectonic mélange.

Supplementary data to this article can be found online at http://dx.doi.org/10.1016/j.lithos.2015.01.029.

Acknowledgments

This study was supported by the National Natural Science Foundation of China (No. 91014002), the Ministry of Education of China (No. B07039) and the China Scholarship Council (No. 201406410042, award to Junpeng Wang for one year's study abroad at University of California, Los Angeles). Ali Polat acknowledges funding from NSERC Discovery Grant 250926. We appreciate Guochun Zhao and an anonymous reviewer for comments that substantially improved the manuscript, and Sun-Lin Chung for his helpful editorial comments. We thank Jianmin Fu, Zhensheng Wang, Ye Yuan, Songjie Wang, Traore Alhousseyni, Xingfu Jiang and Musen Lin from the China University of Geosciences (Wuhan) for helping with the field and laboratory work.

References

Bonin, B., 2007. A-type granites and related rocks: evolution of a concept, problems and prospects. Lithos 97, 1–29.
Chemenda, A., Yang, R., Hsieh, C.H., Groholsky, A., 1997. Evolutionary model for the Taiwan collision based on physical 28 oncordi. Tectonophysics 274, 253–274.
Clemens, J.D., Holloway, J.R., White, A.J.R., 1986. Origin of an A-type granite: experimental constraints. American Mineralogist 71, 317–324.
Clift, P.D., Schouten, H., Draut, A.E., 2003. A general model of arc–continent collision and subduction polarity reversal from Taiwan and the Irish Caledonides. Geological Society, London, Special Publications 219, 81–98.
Collins, W.J., Beams, S.D., White, A.J.R., Chappell, B.W., 1982. Nature and origin of A-type granites with particular reference to southeastern Australia. Contribution to Mineralogy and Petrology 80, 189–200.
Condie, K.C., Kröner, A., 2013. The building blocks of continental crust: evidence for a major change in the tectonic setting of continental growth at the end of the Archean. Gondwana Research 23, 394–402.
Copper, P.A., Taylor, B., 1985. Polarity reversal in the Solomon Islands Arc. Nature 314, 428–430.
Copper, P.A., Taylor, B., 1987. Seismotectonics of New-Guinea: a model for arcreversal following arc–continent collision. Tectonics 6, 53–67.
Corfu, F., Hanchar, J.M., Hoskin, P.W., Kinny, P., 2003. Atlas of zircon textures. Reviews in Mineralogy and Geochemistry 53, 469–500.
Creaser, R.A., Price, R.C., Wormald, R.J., 1991. A-type granites revisited: assessment of residual-source model. Geology 19, 163–166.
Deng, H., Kusky, T.M., Polat, A., Wang, L., Wang, J.P., Wang, S.J., 2013. Geochemistry of Neoarchean mafic volcanic rocks and late mafic dykes in the Zanhuang Complex, Central Orogenic Belt, North China Craton: implications for Geodynamic setting. Lithos 175–176, 193–212.
Deng, H., Kusky, T.M., Polat, A., Wang, J.P., Wang, L., Fu, J.M., Wang, Z.S., Yuan, Y., 2014. Geochronology, mantle source composition and geodynamic constraints on the origin of Neoarchean mafic dikes in the Zanhuang Complex, Central Orogneic Belt, North China Craton. Lithos 205, 359–378.
Dewey, J.F., Bird, J.M., 1970. Mountain belts and the new global tectonics. Journal of Geophysical Research 75, 2625–2647.
Draper, G., Gutiérrez, G., Lewis, J.F., 1996. Thrust emplacement of the Hispaniola peridotite belt: orogenic expression of the mid-Cretaceous Caribbean arc polarity reversal? Geology 24, 1143–1146.
Eby, G.N., 1990. The A-type granitoids: a review of their occurrence and chemical characteristics and speculations on their petrogenesis. Lithos 26, 115–134.
Eby, G.N., 1992. Chemical subdivision of the A-type granitoids: petrogenetic and tectonic implications. Geology 20, 641–644.
Faure, M., Trap, P., Lin, W., Monié, P., Bruguier, O., 2007. Polyorogenic evolution of the Paleoproterozoic Trans-North China Belt: new insights from the Luliangshan–Hengshan–Wutaishan and Fuping massifs. Episodes 30, 96–107.
Fu, J.M., Kusky, T.M., Wang, J.P., Deng, H., Wang, S.J., 2015n. Petrology, geochemistry and geochronology of Haozhuang granite in the Zanhuang Complex, Central Orogenic Belt, North China Craton: constraints on early Precambrian tectonic evolution (in preparation).
Gao, S., Rudnick, R.L., Yuan, H.L., Liu, X.M., Liu, Y.S., Xu, W.L., Ling, W.L., Ayers, J., Wang, X.C., Wang, Q.H., 2004. Recycling lower continental crust in the North China craton. Nature 432, 892–897.
Geng, Y.S., Liu, F.L., Yang, C.H., 2006. Magmatic event at the end of the Archean in eastern Hebei Province and its geological implication. Acta Gologica Sinica 80, 819–833.
Geng, Y.S., Shen, Q.H., Ren, L.D., 2010. Late Neoarchean to early Paleoproterozoic magmatic events and tectonothermal system in the north China craton. Acta Petrologica Sinica 26, 1945–1966 (in Chinese with English abstract).
Geng, Y.S., Du, L.L., Ren, L.D., 2012. Growth and reworking of the early Precambrian continental crust in the North China Craton: constraints from zircon Hf isotopes. Gondwana Research 21, 517–529.
Griffin, W.L., Zhang, A., O'Reilly, S.Y., Ryan, C.G., 1998. Phanerozoic evolution of the lithosphere beneath the Sino-Korean craton-mantle dynamics and plate interactions in East Asia. Geodynamics 27, 107–126.
Han, C.M., Xiao, W.J., Su, B.X., Chen, Z.L., Zhang, X.H., Ao, S.J., Zhang, J.E., Zhang, Z.Y., Wan, B., Song, D.F., Wang, Z.M., 2014. Neoarchean algoma-type banded iron formations from eastern Hebei, north China craton: SHRIMP U–Pb age, origin and tectonic setting. Precambrian Research 251, 212–231.

Hoskin, P.W., Schaltegger, U., 2003. The composition of zircon and igneous and metamorphic petrogenesis. Reviews in Mineralogy and Geochemistry 53, 27–62.
Huang, X.L., Niu, Y.L., Xu, Y.G., Yang, Q.J., Zhong, J.W., 2010. Geochemistry of TTG and TTG-like gneisses from Lushan–Taihua Complex in the southern North China Craton: implications for late Archean crustal accretion. Precambrian Research 182, 43–56.
Jian, P., Kröner, A., Windley, B.F., Zhang, Q., Zhang, W., Zhang, L.Q., 2012. Episodic mantle melting-crustal reworking in the late Neoarchean of the northwestern North China Craton: zircon ages of magmatic and metamorphic rocks from the Yinshan Block. Precambrian Research 222–223, 230–254.
Kemp, A.I.S., Hawkesworth, C.J., 2003. Granitic perspectives on the generation and secular evolution of the continental crust. Treatise on Geochemistry 349–410.
King, P.L., White, A.J.R., Chappell, B.W., Allen, C.M., 1997. Characterization and origin of aluminous A-type granites from the Lachlan Fold Belt, Southeastern Australia. Journal of Petrology 38, 371–391.
King, P.L., Chappell, B.W., Allen, C.M., White, A.J.R., 2001. Are A-type granites the high temperature felsic granites? Evidence from fractionated granites of the Wangrah Suite. Australian Journal of Earth Sciences 48, 501–514.
Konstantinovskaia, E., 2001. Arc–continent collision and subduction reversal in the Cenozoic evolution of the Northwest Pacific: an example from Kamchatka (NE Russia). Tectonophysics 333, 75–94.
Krogh, T.E., 1973. A low contamination method for the hydrothermal decomposition of zircon and extraction of U and Pb for isotopic age determinations. Geochimica et Cosmochimica Acta 37, 485–494.
Kröner, A., Cui, W.Y., Wang, C.Q., Nemchin, A.A., 1998. Single zircon ages from high-grade rocks of the Jianping Complex, Liaoning Province, NE China. Journal of Asian Earth Sciences 16, 519–532.
Kröner, A., Wilde, S.A., Zhao, G.C., O'Brien, P.J., Sun, M., Liu, D.Y., Wan, Y.S., Liu, S.W., Guo, J.H., 2006. Zircon geochronology of mafic dykes in the Hengshan Complex of northern China: evidence for late Palaeoproterozoic rifting and subsequent high-pressure event in the North China Craton. Precambrian Research 146, 45–67.
Kusky, T.M., 2011a. Geophysical and geological tests of tectonic models of the North China Craton. Gondwana Research 20, 26–35.
Kusky, T.M., 2011b. Comparison of results of recent seismic profiles with tectonic models of the North China Craton. Journal of Earth Science 22, 250–259.
Kusky, T.M., Li, J.H., 2003. Paleoproterozoic tectonic evolution of the North China craton. Journal of Asian Earth Sciences 22, 23–40.
Kusky, T.M., Li, J.H., Tucker, R.D., 2001. The Archean Dongwanzi ophiolite complex, North China craton: 2.505-billion-year-old oceanic crust and mantle. Science 292, 1142–1145.
Kusky, T.M., Li, Z.H., Glass, A., Huang, H.A., 2004. Archean ophiolites and ophiolite fragments of the North China Craton. In: Kusky, T.M. (Ed.), Precambrian Ophiolites and Related Rocks: Development in Precambrian Geology. Elsevier 13, pp. 223–274.
Kusky, T.M., Windley, B.F., Zhai, M.G., 2007a. Tectonic evolution of the North China Block: from orogen to craton to orogen. In: Zhai, M.G., Windley, B.F., Kusky, T.M., Meng, Q.R. (Eds.), Mesozoic sub-continental lithospheric thinning under eastern Asia. Geological Society of London, Special Publication 280, pp. 1–34.
Kusky, T.M., Li, J.H., Santosh, M., 2007b. The Paleoproterozoic North Hebei Orogen: North China Craton's collisional suture with Columbia supercontinent. In: Zhai, M.G., Xiao, W.J., Kusky, T.M., Santosh, M. (Eds.), Tectonic evolution of China and adjacent crustal fragments. Gondwana Research 12, pp. 4–28.
Kusky, T.M., Li, X.Y., Wang, Z.S., Fu, J.M., Luo, Z., Zhu, P.M., 2014. Are Wilson Cycles preserved in Archean cratons? A comparison of the North China and Slave cratons. Canadian Journal of Earth Science 51, 297–311.
Lebron, M.C., Perfit, M.R., 1993. Stratigraphic and petrochemical data support subduction polarity reversal of the Cretaceous Caribbean island arc. The Journal of Geology 101, 389–396.
Li, J.H., Kusky, T.M., Huang, X.N., 2002. Archean podiform chromitites and mantle tectonites in ophiolitic mélange, North China Craton: a record of early oceanic mantle processes. GSA TODAY 12, 4–11.
Li, J.H., Yang, C.H., Du, L.L., 2004. Zircon genesis and SHRIMP U–Pb age of the anatetic pegmatite in Pingshan of Hebei province. Progress in Natural Science 14, 774–781 (in Chinese).
Li, J.H., Hou, G.T., Liu, S.J., 2006. The early Precambrian collisional orogenic process and plate tectonics: chance and challenge of Precambrian geology. Advances in Earth Science 21, 77–82 (in Chinese with English abstract).
Li, T.S., Zhai, M.G., Peng, P., Chen, L., Guo, J.H., 2010. Ca. 2.5 billion year old coeval ultramafic–mafic and syenitic dykes in Eastern Hebei: implications for cratonization of the North China Craton. Precambrian Research 180, 143–155.
Liu, D.Y., Page, R.W., Compston, W., Wu, J.S., 1985. U–Pb zircon geochronology of late Archaean metamorphic rocks in the Taihangshan–Wutaishan area, North China. Precambrian Research 27, 85–109.
Liu, D.Y., Shen, Q.H., Zhang, Z.Q., Jahn, B.M., Auvray, B., 1990. Archean crustal evolution in China: U–Pb geochronology of the Qianxi Complex. Precambrian Research 48, 233–244.
Liu, S.W., Zhao, G.C., Wilde, S.A., Shu, G.M., Sun, M., Li, Q.G., Tian, W., Zhang, J., 2006. Th–U–Pb monazite geochronology of the Luliang and Wutai Complexes: constraints on the tectonothermal evolution of the Trans-North China orogen. Precambrian Research 148, 205–224.
Liu, S., Feng, C.X., Zhai, M.G., Hu, R.Z., Gao, S., Lai, S.C., Zou, H.B., Yan, J., 2015. Ca. 2.5 billion year old mafic dykes in western Shandong Province: implications for hybridization between subducted continental crust and the North China Craton, China. Lithos 216-217, 148–157.
Loiselle, M.C., Wones, D.R., 1979. Characteristics of anorogenic granites. Geological Society of America Abstracts with Programs 11, 468.
Lu, S.N., Zhao, G.C., Wang, H.C., Hao, G.J., 2008. Precambrian metamorphic basement and sedimentary cover of the North China Craton: review. Precambrian Research 160, 77–93.
Lu, J.S., Wang, G.D., Wang, H., Chen, H.X., Wu, C.M., 2014. Palaeoproterozoic metamorphic evolution and geochronology of the Wugang block, southeastern terminal of the Trans-North China Orogen. Precambrian Research 251, 197–211.
Ma, X.D., Guo, J.H., Liu, F., Qian, Q., Fan, H.R., 2013. Zircon U–Pb ages, trace elements and Nd–Hf isotopic geochemistry of Guyang sanukitoids and related rocks: implications for the Archean crustal evolution of the Yinshan Block, North China Craton. Precambrian Research 230, 61–78.
McKenzie, D.P., 1969. Speculations on the consequences and causes of plate motions. Geophysical Journal of the Royal Astronomical Society 18, 1–32.
Middelburg, J.J., van der Weijden, C.H., Woittiez, J.R., 1988. Chemical processes affecting the mobility of major, minor and trace elements during weathering of granitic rocks. Chemical Geology 68, 253–273.
Miller, C.F., McDowell, S.M., Mapes, R.W., 2003. Hot and cold granites? Implications of zircon saturation temperatures and preservation of inheritance. Geology 31, 529–532.
Nutman, A.P., Wan, Y.S., Du, L.L., Friend, C.R.L., Dong, C.Y., Xie, H.Q., Wang, W., Sun, H.Y., Liu, D.Y., 2011. Multistage late Neoarchaean crustal evolution of the North China Craton, eastern Hebei. Precambrian Research 189, 43–65.
O'Neil, J., Francis, D., Carlson, R.W., 2011. Implications of the Nuvvuagittuq greenstone belt for the formation of Earth's early crust. Journal of Petrology 52, 985–1009.
Ordóñez-Calderón, J.C., Polat, A., Fryer, B.J., Gagnon, J.E., Raith, J.G., Appel, P.W.U., 2008. Evidence for HFSE and REE mobility during calc-silicate metasomatism, Mesoarchean (~3075 Ma) Ivisaartoq greenstone belt, southern West Greenland. Precambrian Research 161, 317–340.
Panahi, A., Young, G.M., Rainbird, R.H., 2000. Behavior of major and trace elements (including REE) during Paleoproterozoic pedogenesis and diagenetic alteration of an Archean granite near Ville Marie, Quebec, Canada. Geochimica et Cosmochimica Acta 64, 2199–2220.
Patiño Douce, A.E.P., 1997. Generation of metaluminous A-type granites by low pressure melting of calc-alkaline granitoids. Geology 25, 743–746.
Patiño Douce, A.E.P., Beard, J.S., 1995. Dehydration-melting of biotite gneiss and quartz amphibolite from 3 to 15 kbar. Journal of Petrology 36, 707–738.
Peng, P., Zhai, M.G., Guo, J.H., Kusky, T.M., Zhao, T.P., 2007. Nature of mantle source contributions and crystal differentiation in the petrogenesis of the 1.78 Ga mafic dykes in the central North China craton. Gondwana Research 12, 29–46.
Peng, T.P., Wilde, S.A., Fan, W.M., Peng, B.X., 2013. Late Neoarchean potassic high Ba–Sr granites in the Taishan granite-greenstone terrane: petrogenesis and implications for continental crustal evolution. Chemical Geology 344, 23–41.
Peng, P., Wang, X.P., Windley, B.F., Guo, J.H., Zhai, M.G., Li, Y., 2014. Spatial distribution of ~1950–1800 Ma metamorphic events in the North China Craton: implications for tectonic subdivision of the craton. Lithos 202–203, 250–266.
Polat, A., Hofmann, A.W., 2003. Alteration and geochemical patterns in the 3.7–3.8 Ga Isua greenstone belt, West Greenland. Precambrian Research 126, 197–218.
Polat, A., Herzberg, C., Munker, C., Rodgers, R., Kusky, T., Li, J., Fryer, B., Delaney, J., 2006. Geochemical and petrological evidence for a suprasubduction zone origin of Neoarchean (ca. 2.5 Ga) peridotites, central orogenic belt, North China craton. Geological Society of America Bulletin 118, 771–784.
Polat, A., Fryer, B.J., Samson, I.M., Weisener, C., Appel, P.W.U., Frei, R., Windley, B.F., 2012. Geochemistry of ultramafic rocks and hornblendite veins in the Fiskenæsset layered anorthosite complex, SW Greenland: evidence for hydrous upper mantle in the Archean. Precambrian Research 214–215, 124–153.
Polat, A., Kusky, T.M., Li, J.H., Fryer, B., Kerrich, R., Patrick, K., 2005. Geochemistry of Neoarchean (ca. 2.55–2.50 Ga) volcanic and ophiolitic rocks in the Wutaishan greenstone belt, central orogenic belt, North China craton: Implications for geodynamic setting and continental growth. Geol. Soc. Am. Bull. 117, 1387–1399.
Pubellier, M., Bader, A.G., Rangin, C., Deffontaines, B., Quebral, R., 1999. Upper plate deformation induced by subduction of a volcanic arc: the Snellius Plateau (Molucca Sea, Indonesia and Mindanao, Philippines). Tectonophysics 304, 345–368.
Rubatto, D., 2002. Zircon trace element geochemistry: partitioning with garnet and the link between U–Pb ages and metamorphism. Chemical Geology 184, 123–138.
Santosh, M., 2010. Assembling North China Craton within the Columbia supercontinent: the role of double-sided subduction. Precambrian Research 178, 149–167.
Skjerlie, K.P., Johnston, A.D., 1993. Fluid-absent melting behaviour of an F-rich tonalite gneiss at mid-crustal pressures: implications for the generation of anorogenic granites. Journal of Petrology 34, 785–815.
Sun, S.S., McDonough, W.F., 1989. Chemical and isotopic 36oncordia36 of oceanic basalts: implications for mantle composition and processes. In: Saunders, A.D., Norry, M.J. (Eds.), Magmatism of the ocean basins, Geological Society of London Special Publication 42, pp. 313–345.
Tang, J., Zheng, Y.F., Wu, Y.B., Gong, B., Liu, X.M., 2007. Geochronology and geochemistry of metamorphic rocks in the Jiaobei terrane: constraints on its tectonic affinity in the Sulu orogen. Precambrian Research 152, 48–82.
Teng, L.S., Lee, C., Tsai, Y., Hsiao, L.Y., 2000. Slab breakoff as a mechanism for flipping of subduction polarity in Taiwan. Geology 28, 155–158.
Tobisch, O.T., Paterson, S.R., 1990. The Yarra granite: an intradeformational pluton associated with ductile thrusting, Lachlan Fold Belt, Southeastern Australia. Geological Society of America Bulletin 102, 693–703.
Trap, P., Faure, M., Lin, W., Monié, P., Meffre, S., Melleton, J., 2009. The Zanhuang Massif, the second and eastern suture zone of the Paleoproterozoic Trans-North China Orogen. Precambrian Research 172, 80–98.
Trap, P., Faure, M., Lin, W., Breton, N.L., Monié, P., 2012. Paleoproterozoic tectonic evolution of the Trans-North China Orogen: toward a comprehensive model. Precambrian Research 222–223, 191–211.

Ustaszewski, K., Wu, Y.M., Suppe, J., Huang, H.H., Chang, C.H., Carena, S., 2012. Crust–mantle boundaries in the Taiwan-Luzon arc–continent collision system determined from local earthquake tomography and 1D models: implications for the mode of subduction polarity reversal. Tectonophysics 578, 31–49.
Vignaroli, G., Faccenna, C., Jolivet, L., Piromallo, C., Rossetti, F., 2008. Subduction polarity reversal at the junction between the Western Alps and the Northern Apennines, Italy. Tectonophysics 450, 34–50.
Wan, Y.S., Liu, D.Y., Wang, S.Y., Zhao, X., Dong, C.Y., Zhou, H.Y., Yin, X.Y., Yang, C.X., Gao, L.Z., 2009. Early Precambrian crustal evolution in the Dengfeng area, Henan Province (eastern China): constraints from geochemistry and SHRIMP U–Pb zircon dating. Acta Geologica Sinica 83, 982–999 (in Chinese with English abstract).
Wan, Y.S., Liu, D.Y., Wang, S.J., Dong, C.Y., Yang, E.X., Wang, W., Zhou, H.Y., Ning, Z.G., Du, L.L., Yin, X.Y., Xie, H.Q., Ma, M.Z., 2010. Juvenile magmatism and crustal recycling at the end of the Neoarchean in western Shandong Province, North China Craton: evidence from SHRIMP zircon dating. American Journal of Sciences 310, 1503–1552.
Wan, Y.S., Dong, C.Y., Liu, D.Y., Kröner, A., Yang, C.H., Wang, W., Du, L.L., Xie, H.Q., Ma, M.Z., 2012. Zircon ages and geochemistry of Late Neoarchean syenogranites in the North China Craton: a review. Precambrian Research 222–223, 265–289.
Wang, J.P., Kusky, T.M., Polat, A., Wang, L., Deng, H., Wang, S.J., 2013a. A late Archean tectonic mélange belt in the Central Orogenic Belt, North China Craton. Tectonophysics 608, 929–946.
Wang, W., Liu, S.W., Santosh, M., Bai, X., Li, Q.G., Yang, P.T., Guo, R.R., 2013b. Zircon U–Pb–Hf isotopes and whole-rock geochemistry of granitoid gneisses in the Jianping gneissic terrane, Western Liaoning Province: constraints on the Neoarchean crustal evolution of the North China Craton. Precambrian Research 224, 184–221.
Wang, G.D., Wang, H., Chen, H.X., Lu, J.S., Wu, C.M., 2014a. Metamorphic evolution and zircon U–Pb geochronology of the Mts. Huashan amphibolites: insights into the Palaeoproterozoic amalgamation of the North China Craton. Precambrian Research 245, 100–114.
Wang, Q.Y., Zheng, J.P., Pan, Y.M., Dong, Y.J., Liao, F.X., Zhang, Y., Zhang, L., Zhao, G., Tu, Z.B., 2014b. Archean crustal evolution in the southeastern North China Craton: new data from the Huoqiu Complex. Precambrian Research 255, 294–315.
Wang, W., Zhai, M.G., Li, T.S., Santosh, M., Zhao, L., Wang, H.Z., 2014c. Archean-Paleoproterozoic crustal evolution in the eastern North China Craton: zircon U–Th–Pb and Lu–Hf evidence from the Jiaobei terrane. Precambrian Research 241, 146–160.
Wang, X., Zhu, W.B., Ge, R.F., Luo, M., Zhu, X.Q., Zhang, Q.L., Wang, L.S., Ren, X.M., 2014d. Two episodes of Paleoproterozoic metamorphosed mafic dykes in the Lvliang Complex: implications for the evolution of the Trans-North China Orogen. Precambrian Research 243, 133–148.
Watson, E.B., Harrison, T.M., 1983. Zircon saturation revisited: temperature and composition effects in a variety of crustal magma types. Earth and Planetary Science Letters 64, 295–304.
Whalen, J.B., Currie, K.L., Chappell, B.W., 1987. A-type granites: geochemical characteristics, discrimination and petrogenesis. Contribution to Mineralogy and Petrology 95, 407–419.
Wilde, S.A., Cawood, P.A., Wang, K.Y., 1997. The relationship and timing of granitoid evolution with respect to felsic volcanism in the Wutai Complex, North China Craton. Proceedings of the 30th International Geological Congress, Beijing, vol. 17. VSP International Science Publishers, Amsterdam, pp. 75–87.
Wilde, S.A., Cawood, P.A., Wang, K.Y., Nemchina, A.A., 2005. Granitoid evolution in the Late Archean Wutai Complex, North China Craton. Journal of Asian Earth Sciences 24, 597–613.
Wong, J., Sun, M., Xing, G., Li, X.H., Zhao, G., Wong, K., Wu, F., 2011. Zircon U–Pb and Hf isotopic study of Mesozoic felsic rocks from eastern Zhenjiang, South China: geochemical contrast between Yangtze and Cathaysia blocks. Gondwana Research 19, 244–259.
Wu, Y.B., Zheng, Y.F., 2004. Genesis of zircon and its constraints on interpretation of U–Pb age. Chinese Science Bulletin 49, 1554–1569.
Wu, F.Y., Sun, D.Y., Li, H., Jahn, B.M., Wilde, S., 2002. A-type granites in northeastern China: age and geochemical constraints on their petrogenesis. Chemical Geology 187, 143–173.
Wu, M.L., Zhao, G.C., Sun, M., Yin, C.Q., Li, S.Z., Tam, P.Y., 2012. Petrology and P–T path of the Yishui mafic granulites: implications for tectonothermal evolution of the Western Shandong Complex in the Eastern Block of the North China Craton. Precambrian Research 222–223, 312–324.
Wu, M.L., Zhao, G.C., Sun, M., Bao, Z.A., Tam, P.Y., He, Y.H., 2014. Tectonic affinity and reworking of the Archaean Jiaodong Terrane in the Eastern Block of the North China Craton: evidence from LA–ICP–MS U–Pb zircon ages. Geological Magazine 151, 365–371.
Xiao, L.L., Wang, G.D., 2011. Zircon U–Pb dating of metabasic rocks in the Zanhuang metamorphic complex and its geological significance. Acta Petrologica et Mineralogica 30, 781–794 (in Chinese with English abstract).
Xiao, L.L., Liu, F.L., Chen, Y., 2014. Metamorphic P–T-t paths of the Zanhuang metamorphic complex: implications for the Paleoproterozoic evolution of the Trans-North China Orogen. Precambrian Research 255, 216–235.
Yang, J.H., Wu, F.Y., Chung, S.L., Wilde, S.A., Chu, M.F., 2006. A hybrid origin for the Qianshan A-type granite, northeast China: geochemical and Sr–Nd–Hf isotopic evidence. Lithos 89, 89–106.
Yang, J.H., Wu, F.Y., Wilde, S.A., Zhao, G.C., 2008. Petrogenesis and geodynamics of Late Archean magmatism in eastern Hebei, eastern North China Craton: geochronological, geochemical and Nd–Hf isotopic evidence. Precambrian Research 167, 125–149.
Yang, C.H., Du, L.L., Ren, L.D., Song, H.X., Wan, Y.S., Xie, H.Q., Liu, Z.X., 2011a. The age and petrogenesis of the Xuting granite in the Zanhuang Complex, Hebei Province: constraints on the structural evolution of the Trans-North China Orogen, North China Craton. Acta Petrologica Sinica 27, 1003–1016 (in Chinese with English abstract).
Yang, C.H., Du, L.L., Ren, L.D., Song, H.X., Wan, Y.S., Xie, H.Q., Liu, Z.X., 2011b. Petrogenesis and geodynamic setting of Jiandeng potassic granite at the end of the Neoarchean in Zanhuang Complex, North China Craton. Earth Science Frontiers 18, 62–78 (in Chinese with English abstract).
Yang, C.H., Du, L.L., Ren, L.D., Song, H.X., Wan, Y.S., Xie, H.Q., Geng, Y.S., 2013. Delineation of the ca. 2.7 Ga TTG gneisses in the Zanhuang Complex, North China Craton and its geological implications. Journal of Asian Earth Sciences 72, 178–189.
Yin, C.Q., Zhao, G.C., Wei, C.J., Sun, M., Guo, J.H., Zhou, X.W., 2014. Metamorphism and partial melting of high-pressure pelitic granulites from the Qianlishan Complex: constraints on the tectonic evolution of the Khondalite Belt in the North China Craton. Precambrian Research 242, 172–186.
Zhai, M.G., Santosh, M., 2011. The early Precambrian odyssey of the North China Craton: a synoptic overview. Gondwana Research 20, 6–25.
Zhang, C.L., Li, Z.X., Li, X.H., Yu, H.F., Ye, H.M., 2007a. An early Paleoproterozoic high-K intrusive complex in southwestern Tarim Block, NW China: age, geochemistry, and tectonic implications. Gondwana Research 12, 101–112.
Zhang, H.F., Parrish, R., Zhang, L., Xu, W.C., Yuan, H.L., Gao, S., Crowley, Q.G., 2007b. A-type granite and adakitic magmatism association in Songpan–Garze fold belt, eastern Tibetan Plateau. Implication for lithospheric delamination. Lithos 97, 323–335.
Zhang, J., Zhao, G.C., Li, S.Z., Sun, M., Liu, S.W., Wilde, S.A., Kroner, A., Yin, C.Q., 2007c. Deformation history of the Hengshan Complex: implications for the tectonic evolution of the Trans-North China Orogen. Journal of Structural Geology 29, 933–949.
Zhang, J., Zhao, G.C., Li, S.Z., Sun, M., Liu, S.W., Yin, C.Q., 2009. Polyphase deformation of the Fuping Complex, Trans-North China Orogen: structures, SHRIMP U–Pb zircon ages and tectonic implications. Journal of Structural Geology 31, 177–193.
Zhang, H.F., Zhai, M.G., Santosh, M., Diwu, C.R., Li, S.R., 2011. Geochronology and petrogenesis of Neoarchean potassic meta-granites from Huai'an Complex: implications for the evolution of the North China Craton. Gondwana Research 20, 82–105.
Zhang, J., Zhao, G.C., Shen, W.L., Li, S.Z., Sun, M., Chan, L.S., Liu, S.W., 2012. Structural and aeromagnetic studies of the Wutai Complex: implications for the tectonic evolution of the Trans-North China Orogen. Precambrian Research 222–223, 212–229.
Zhang, J., Zhang, H.F., Lu, X.X., 2013. Zircon U–Pb age and Lu–Hf isotope constraints on Precambrian evolution of continental crust in the Songshan area, the south-central North China Craton. Precambrian Research 226, 1–20.
Zhao, G.C., 2001. Paleoproterozoic assembly of the North China Craton. Geological Magazine 138, 87–91.
Zhao, G.C., 2009. Metamorphic evolution of major tectonic units in the basement of the North China Craton: key issues and discussion. Acta Petrologica Sinica 25, 1772–1792.
Zhao, G.C., Guo, J.H., 2012. Precambrian geology of China: preface. Precambrian Research 222–223, 1–12.
Zhao, G.C., Zhai, M.G., 2013. Lithotectonic elements of Precambrian basement in the North China Craton: review and tectonic implications. Gondwana Research 23, 1207–1240.
Zhao, G.C., Wilde, S.A., Cawood, P.A., Lu, L.Z., 1999. Thermal evolution of two textural types of mafic granulites in the North China Craton: evidence for both mantle plume and collisional tectonics. Geological Magazine 136, 223–240.
Zhao, G.C., Wilde, S.A., Cawood, P.A., Sun, M., 2001. Archean blocks and their boundaries in the North China Craton: lithological, geochemical, structural and P–T path constraints and tectonic evolution. Precambrian Research 107, 45–73.
Zhao, G.C., Wilde, S.A., Cawood, P.A., Sun, M., 2002. SHRIMP U–Pb zircon ages of the Fuping Complex: implication for late Archean to Paleoproterozoic accretion and assembly of the North China Craton. American Journal of Science 302, 191–226.
Zhao, G.C., Sun, M., Wilde, S.A., Li, S.Z., 2005. Late Archean to Paleoproterozoic evolution of the North China Craton: key issues revisited. Precambrian Research 136, 177–202.
Zhao, G.C., Wilde, S.A., Sun, M., Guo, J.H., Kröner, A., Li, S.Z., Li, X.P., Zhang, J., 2008. SHRIMP U–Pb zircon geochronology of the Huai'an Complex: constraints on Late Archean to Paleoproterozoic magmatic and metamorphic events in the Trans-North China Orogen. American Journal of Science 308, 270–303.
Zhao, G.C., Cawood, P.A., Wilde, S.A., Sun, M., Zhang, J., He, Y.H., Yin, C.Q., 2012. Amalgamation of the North China Craton: key issues and discussion. Precambrian Research 222–223, 55–76.
Zhou, Y.Y., Zhao, T.P., Wang, C.Y., Hu, G.H., 2011. Geochronology and geochemistry of 2.5 to 2.4 Ga granitic plutons from the southern margin of the North China Craton: implications for a tectonic transition from arc to post-collisional setting. Gondwana Research 20, 171–183.